UNIVERSITÀ DEL PIEMONTE ORIENTALE

School of Medicine

HEALTH SCIENCES DEPARTMENT

Master degree in medical biotechnologies

Master thesis

REGENERATIVE POTENTIAL OF MATRIX BOUND NANOVESICLES (MBVs) FROM DECELLULARIZED BOVINE PERICARDIUM

Mentor:

Prof. Francesca Boccafoschi

Firmato digitalmente da Francesca Boccafoschi
Data: 27.06.2024 00:19:45 CEST
Organizzazione: UNIVERSITA' DEGLI STUDI DEL PIEMONTE ORIENTALE/01943490027

Candidate:

Carolina Di Varsavia

Matricula n. 20023413

Academic year 2023-2024

INDEX

1. SUMMARY

Matrix-bound nanovesicles (MBVs) represent a novel class of extracellular vesicles that exhibit a unique affinity for extracellular matrix proteins (ECM), with a tissue-specific cargo capable of mimicking the biological activity of the source extracellular matrix. These MBVs have garnered interest in regenerative medicine due to their potent cell signaling and immune-modulating properties. Up to now MBVs have only been isolated in urinary bladder matrix, submucosa of the small intestine, dermis, brain, heart, ovary, pancreas, and muscle. Thus, the aim of this research aimed to isolate and identify MBVs in decellularized bovine pericardium extracellular matrix and characterize their protein content, crucial for their biological functionality.

In this study, the primary goal was to isolate MBVs from decellularized bovine pericardium ECM and characterize their composition and biological functionality. This involved the employment of different analytical techniques including nanoparticle tracking assay (NTA), for the determination of MBV size distribution, while transmission electron microscopy (TEM) provided valuable insights into their morphological features, and proteomic analysis to elucidate the protein and cytokine cargo encapsulated within these MBVs, as well as assessing their effects on cellular behavior and immune response modulation, including proliferation and differentiation. Furthermore, cytocompatibility assays confirmed the biocompatibility of MBVs, suggesting their potential for therapeutic applications in tissue regeneration.

The results of this study demonstrated the successful isolation and characterization of MBVs from decellularized bovine pericardium ECM. NTA and TEM analyses revealed the size and morphology of the MBVs, while proteomic analysis identified a diverse array of proteins and cytokines within their cargo that replicate some of the contents found in their host cells, indicating a significant biological impact, and highlighting their promise for regenerative medicine applications. In vitro experiments demonstrated the ability of MBVs to modulate cellular behavior, including promoting cell proliferation, and modulating immune responses. These findings open the door for further research, exploring their abilities to modulate the immune system, promote blood vessel formation, encourage stem cell specialization, and facilitate wound healing.

2. INTRODUCTION

2.1 Regenerative Medicine

Regenerative medicine is a rapidly growing field that aims to restore or replace damaged tissues and organs that have been damaged by age, disease, trauma, or congenital issues. This dynamic field harnesses a multitude of cutting-edge approaches, including tissue engineering, where biologically compatible scaffolds are implanted in the body at the site where new tissue is to be formed. Cellular and gene therapies through which scientists and clinicians are developing and refining their ability to prepare harvested cells to be injected into patients to repair diseased or damaged tissues and finally, medical devices and artificial organs, with the strategy of replacing organs or tissues from a donor, especially when suitable donor organs are not available. The combination of these approaches can amplify the natural healing process [1] [**Fig.1**]. It goes beyond disease management to finding and seeking treatments to repair, heal, and restore the body to a healthy and functional state. Regenerative medicine uses innovative technologies to address the unmet basic needs of populations [2]. In the last three decades, the field of tissue engineering and regenerative medicine has emerged, where the collaborative efforts of scientists, engineers, and medical professionals converge to create biomimetic structures that mimic natural tissues for research and therapeutic purposes. Much of this work has translated into innovative treatments, particularly in the area of skin replacement and, to a lesser extent, cartilage repair. Tissue engineering is a new field that uses living cells, biocompatible materials, appropriate biochemistry, and physic, as well as combinations of these, to create tissue-like structures. Primary to these advancements are biomaterials, matrices seamlessly integrated into the body to foster tissue repair and regeneration. Whether natural or synthetic, biomaterials provide a scaffold for cell growth, deliver crucial factors for tissue development, and create an environment favorable to regeneration [3].

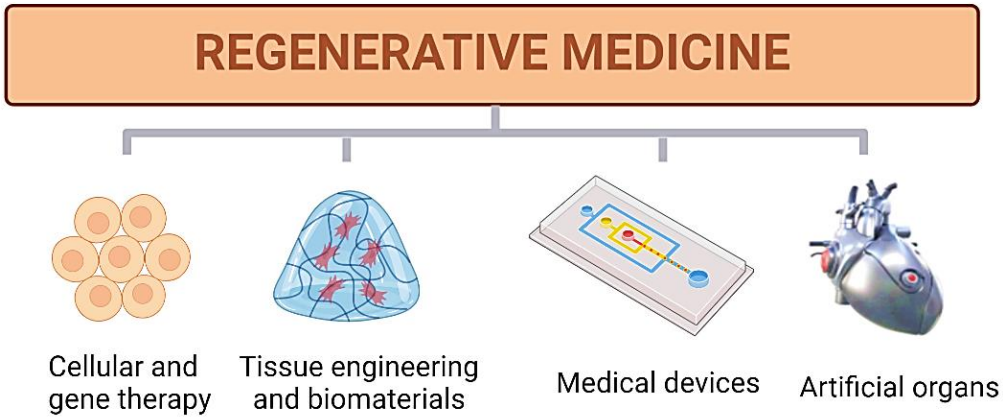

Figure 1 *Key classes in Regenerative Medicine: Cellular and gene therapy, tissue engineering and biomaterials, medical devices and artificial organs. These approaches aim to go beyond traditional disease management, striving to repair, heal and restore the body to a healthy and functional state through innovative technologies.*

2.2 Biomaterials

Biomaterials are any material, structure or surface associated with biological systems. According to the recent definition, a biological material is "*a form that can perform a curative or restorative action by interacting with the living system*" [4]. Biomaterials play a critical role in regenerative medicine, supporting the repair and regeneration of damaged tissues and organs and are classified based on different criteria, including their chemical and physical composition, biodegradability, and source. This classification helps guiding the selection of biomaterials based on their intended use and desired outcomes in regenerative medicine applications. The biomaterials can be categorized into two main classes: natural and synthetic, both compatible with the human tissues [5] [**Fig.2**]. Natural biomaterials are derived from biological sources, such as collagen, chitosan, and silk. They offer advantages such as biocompatibility, bioactivity, and cell adhesion properties [6]. On the other hand, synthetic biomaterials are man-made and typically composed of polymers or ceramics. They can be quite easily engineered to have specific properties and functionalities, such as controllable degradation rates, mechanical strength, and surface modifications. This allows for the customization of biomaterials to suit specific applications and tissue engineering needs. By understanding the distinct characteristics of natural and synthetic biomaterials, researchers and clinicians can make informed decisions regarding their use in regenerative medicine [7]. For example, natural biomaterials may be preferred in cases a more biologically active environment is desired, such as promoting cell attachment and tissue integration [8]. In contrast, synthetic biomaterials may be preferred when precise control over material properties is needed, such as tailoring mechanical strength or degradation rates. By

combining the unique properties of both natural and synthetic biomaterials, researchers can create composite materials that harness the advantages of each component. These composites can have enhanced biological and mechanical properties, making them suitable for a wide range of regenerative medicine applications [5]. The research aims to improve biomaterials in traditional applications and obtain new and effective biomaterials for various advanced applications, including biomedical materials, therapeutics or health problems [4], [6], [8], [9]. In the field of regenerative medicine, the cellular microenvironment influences cell adhesion, migration, differentiation, proliferation, and communication on or within the extracellular matrix (ECM) and biological factors. In most cases, the best biomaterials for tissue engineering and regenerative medicine aim to provide a favorable microenvironment for cells by mimicking their ECM [10].

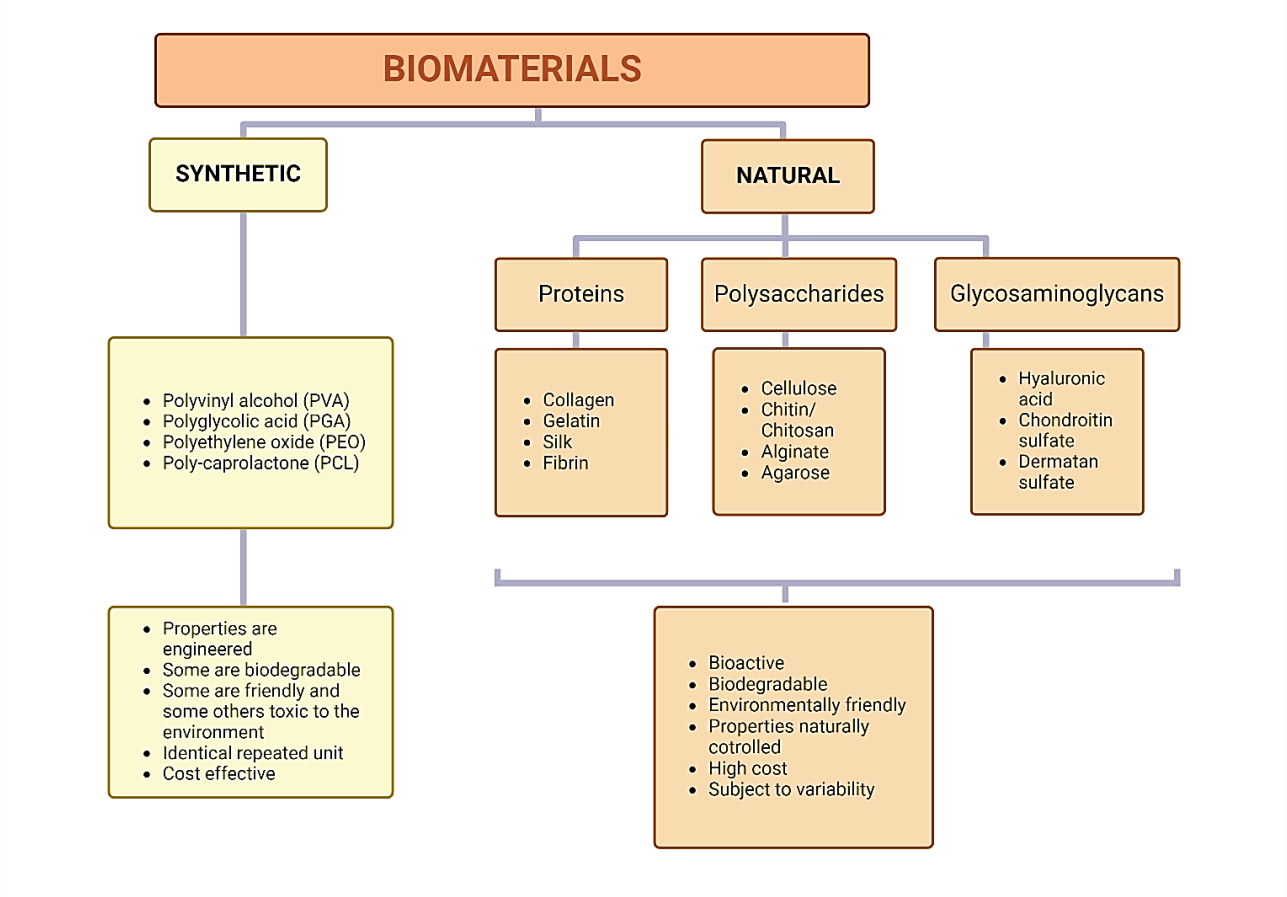

Figure 2 *Comprehensive classification of Biomaterials, divided into synthetic and natural categories, each with distinct materials and characteristics. Synthetic biomaterials such as PVA and PGA, are engineered with consistent properties and generally cost-effective while natural biomaterials, including proteins, polysaccharides and glycosaminoglycans, are bioactive and biodegradable but are more expensive and subject to natural variability.*

2.2.1 Synthetic Biomaterials

Synthetic biomaterials are engineered materials designed to mimic or enhance the properties of natural tissues. They offer precise control over composition, structure, and properties, making them suitable for various biomedical applications. The class of synthetic polymers includes biodegradable, bioabsorbable, and synthetically redesigned so they can be adapted to any application [6], [11]. The main difference between synthetic and natural polymers is that the scaffold can be synthesized and modified in a controlled manner to achieve specific properties or stability. These polymers include polyvinyl alcohol (PVA), polyethylene oxide (PEO), poly("-caprolactone) (PCL), polyurethane (PU), polylactic acid (PLA), polyvinylpyrrolidone (PVP), and polyglycolic acid (PGA) [11], [12]. The chemical properties, mechanics and kinematics of these materials can be adjusted to the type of application required. Mechanical strength, degradation rate and surface properties, can be tailored to a variety of biological applications, and are manufactured under management practices [6], [12]. They are more consistent and sustainable and provide reproducibility. Some synthetic biomaterials exhibit excellent long-term durability and resistance to degradation, making them suitable for applications requiring long-term deployment. Unlike natural materials, some synthetic materials are non-biodegradable and can have detrimental environmental impacts. Although synthetic biomaterials can be manufactured into scaffolds with fully interconnected pores, some classes such as poly (α-hydroxy esters), may produce acidic degradation products that can alter the pH of their surrounding tissues. Nevertheless, synthetic materials typically do not carry a high risk of inducing an immune response because of the lack of biologically functional domains but this is also a limitation because this lack does not guide the natural response of the body to sustain the tissue regeneration [13].

2.2.2 Natural Biomaterials

Natural biomaterials are biological materials extracted from animals or plants with physical and chemical properties suitable for various biomedical applications [6]. Natural biomaterials should be non-immunogenic, biocompatible, biodegradable, easy to produce, readily available, inexpensive, sterilizable, and renewable [14], [15]. They can be distinguished as those derived from *proteins* (for example, collagen, gelatin, silk, and fibrin); *polysaccharides* (cellulose, chitin/chitosan, alginate, and agarose), or *glycosaminoglycans* (hyaluronic acid, chondroitin sulfate, dermatan sulfate, heparan sulfate and keratan sulfate). Natural biomaterials, including collagen, hyaluronic acid, and chitosan, have been widely used in the development of medical devices, tissue engineering applications, regenerative medicine approaches, and drug delivery systems. These molecules are structural arrangements characterized by a series of repeating units or monomers (mainly amino acids or monosaccharides) joined to form peptides and polysaccharides [16].

Due to their intrinsic structural and biological properties, including cell proliferation, adhesion, and non-toxicity to native healthy tissues similar to the ECM, natural biomaterials are widely used in tissue engineering, supporting cell adhesion, differentiation, oxygen and nutrient transport, resulting in the structural and functional recovery [11], [15].

However, the uneven mechanical properties and biostability of natural biomaterials limit their applications in tissue engineering. Therefore, the creation of compounds by combining natural and synthetic components is considered a valid method to improve medicines by achieving high biological functions, as well as mechanical and biological properties, which have been proven in various studies [16]. To overcome these limitations, the use of biomaterials derived from decellularized extracellular matrix (dECM) has emerged as an important solution. Decellularization is a technique that has revolutionized the use of biomaterials in regenerative medicine and opened up new possibilities for tissue engineering and organ transplantation, as it allows for the use of native, patient-specific biomaterials that can be tailored to meet the specific needs of the individual [9], [10].

2.3 Decellularization

ECM is a complex network of proteins and polysaccharides with a tissue-specific structure and composition that is an important part of the stem cell niche [17]. Due to their unique properties and functions, ECM molecules, such as collagens, hyaluronic acid and proteoglycans, play a vital role in the field of regenerative medicine. Functioning as the backbone of tissue architecture, ECM molecules provide essential structural support to cells and tissues, preserving tissue integrity and organization. In regenerative medicine, ECM components are often used to create scaffolds that mimic the natural ECM, providing a framework for cell attachment, proliferation, and differentiation. By incorporating ECM components into scaffolds, regenerative medicine aims to create an environment that promotes cell attachment and movement, essential for tissue regeneration [9], [18], [19], [20]. ECM molecules are biocompatible and well-tolerated by the body, making them ideal candidates for use in tissue engineering and regenerative medicine applications. Their natural composition and properties make them suitable for promoting tissue regeneration without eliciting adverse immune responses.

At the same time, the ECM is a source and site for the active exchange of ions, nutrients, water, metabolites, and signals. In this way, the ECM becomes an environment for tissue-resident cells to connect, communicate, interact, control cell dynamics and behavior, and contribute to the maintenance of tissue and signaling functions. Since the complexity of the native ECM cannot be easily replicated using synthetic materials, an increasing number of studies have examined the use of

scaffolds derived from decellularized tissues for cell culture and delivery [21]. Bioscaffolds derived from the ECM of decellularized tissues can simulate the complex extracellular microenvironment while maintaining the structural, biomechanical, and compositional properties unique to native ECM [19]. One of the key approaches in regenerative medicine is Decellularization, a process that involves the removal of cellular components from tissues while preserving the ECM [22]. Decellularization protocols combine physical and chemical treatments for removing cellular antigens. Physical methods can include freeze-thawing, mechanical agitation or sonication. Chemical methods can include treatments with ionic or non-ionic detergents and enzymes able to disrupt cell membranes, waste products (primarily DNA) as well as intercellular and extracellular adhesion [23].

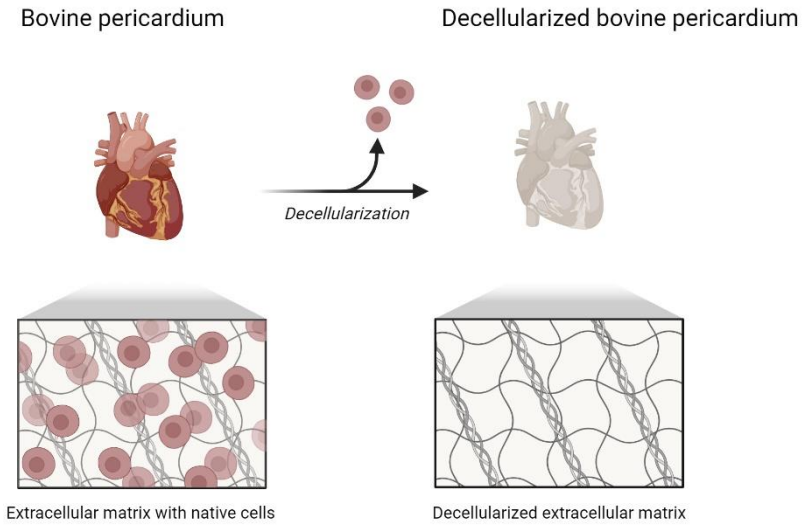

Figure 3 *Decellularization of Bovine Pericardium: An in-depth cellular removal process and the structural characteristics of resultant Extracellular Matrices, able to mimic and retain the native architecture of the ECM.*

This process provides several advantages over other methods in regenerative medicine. Firstly, decellularization allows for the creation of transplantable tissues and organs without the need for immunosuppression [24]. This is because decellularized tissues do not contain donor cells, reducing the risk of immune rejection by the recipient [25]. Additionally, decellularization retains the native architecture and composition of the ECM, providing an optimal environment for cell attachment, migration, and differentiation and the best scaffold for tissue engineering is dECM from the target tissue.

Decellularization allows researchers to obtain a natural, cell-free ECM characterized by proper 3D organization and appropriate molecular structure [26]. Decellularized tissues often contain biological molecules such as growth factors and cytokines that can promote cell growth. Therefore, benefits associated with dECM are often related to improved functionality and use as an adjunct to tissue repair and improved mechanical/biological properties for use. By utilizing the decellularization process, regenerative medicine can address the limited supply of organ transplants and provide alternative strategies for treatment. This can lead to improved patient outcomes and a reduction in the demand for organ donors [23]. The use of ECM biomaterials has shown beneficial results in wound healing [27], repair of the nervous system [28], treatment of liver fibrosis [20], treatment of myocardial infarction [29], cartilage repair [30], tendon repair [31], hernia and other applications [9], [32], [33]. Currently, the precise mechanisms by which ECM biomaterials can direct cellular mechanisms and the immune system to promote tissue regeneration, especially in pathological cases, are not fully understood [34]. The application of decellularization in these different tissues and organs highlights its versatility and potential to address a wide range of medical needs. While the decellularization process holds immense potential, it is not without challenges. One of the primary challenges is achieving complete cell removal while preserving the native ECM structure. Additionally, ensuring the elimination of cellular remnants, such as DNA and cellular debris, requires careful processing, validation methods and the variability that can exist between different animals or tissue sources. Again, loss of specific cell functions, variability in decellularization protocols, because there is no standard protocol for cell removal. Research in this field is focused on the development of the necessary methods and technologies, but then moved on to implement biotechnological approaches. Overcoming these challenges is crucial to ensuring the efficacy and safety of decellularized tissues and organs for clinical use [35].

The accepted hypothesis is that a better biological performance is related to the complex structure of the dECM. The dECM contains key structural components of the ECM, such as collagen, glycoproteins, and proteoglycans, and the ability of dECM biomaterials to not simply escape the immune system but interact with it and is known as immunomodulation, the ability to drive immune cells from an inflammatory state to a healing state. In recent years, studies have shown that most of these healing and immunomodulatory mechanisms are driven by exposure to dECM biodegradation products, which are often obtained by degradation of the dECM matrix resulting from decellularization processes, enzymatic digestion and/or solubilization methods used to obtain dECM biomaterials such as hydrogels, which is mostly based on pepsin solubilization, less invasive and adapt to more irregular shapes than implanted scaffolds, or electrospun scaffolds with the advantage that the layered microfibers can be designed to approximate the architecture of ECM networks, or,

again, bioprinted scaffolds designed to replicate the different characteristics of layered ECM structures and bioinks [9]. This allows the expression of highly active biological molecules trapped in the matrix, such as matrixins, chemokines, cytokines, peptides and matrix-bound nanovesicles (MBVs), recently identified as an important contributor to the healing and immunomodulating potential of ECM biomaterials.

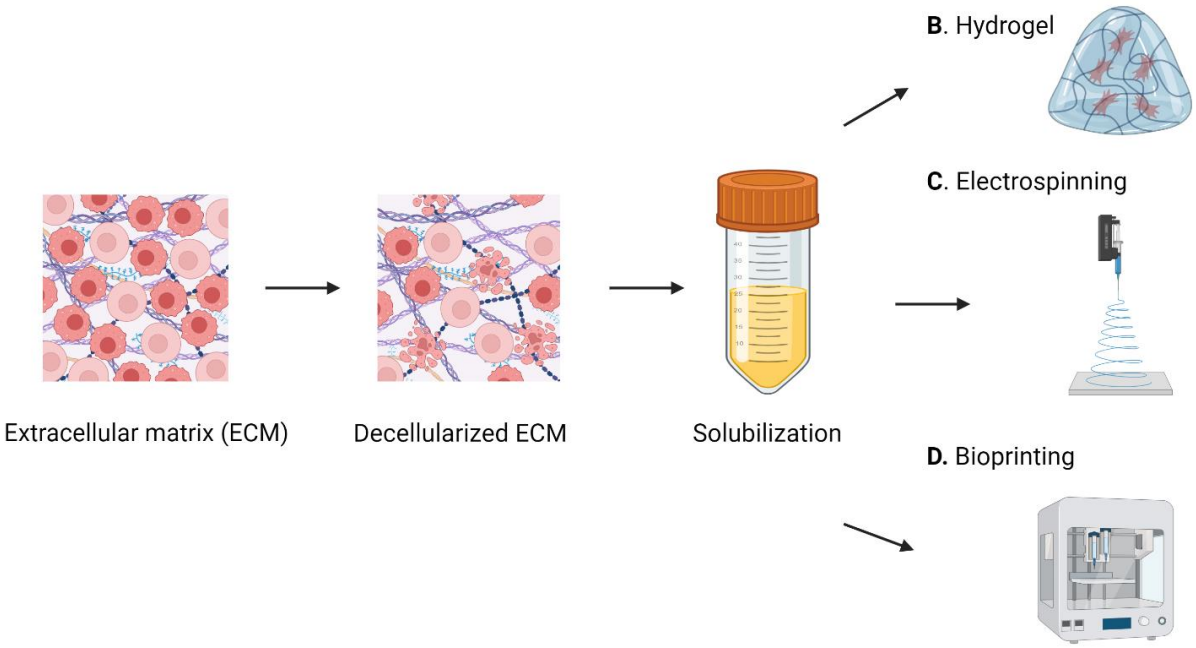

Figure 4 *Decellularization and Processing of Extracellular Matrix: Native ECM is first decellularized and solubilized. The resulting solubilized ECM can be utilized in various biomedical applications including the formation of Hydrogels* ***(B)****: Electrospinning* ***(C)****: polymer fibers can be electrostatically deposited to match ECM fiber and Bioprinting, particularly useful for tissues with multiple layers* ***(D)****. Each offering distinct structural and functional benefits for tissue engineering and regenerative medicine.*

2.4 Matrix-Bound Nanovesicles

A new type of extracellular vesicles (EVs), the matrix-bound nanovesicles (MBVs), has recently been discovered and gained attention in the field of regenerative medicine. MBVs are nano-scale vesicles secreted by cells and embedded within the extracellular matrix, tightly adhered to the collagen network of ECM. MBVs are important due to their unique localization within the extracellular matrix, which sets them apart from other EVs which include exosomes, microvesicles, and apoptotic bodies, [**Fig.5**]. MBVs range in size from 20 to 400 nm and contain a variety of intravesicular proteins and miRNAs as well as lipids. They are similar in size and shape to exosomes and microvesicles but are distinct in their origin, markers, contents, and roles. Furthermore, since MBVs are found to adhere to the ECM unlike other EVs found in body fluids, their isolation also becomes more difficult and must be standardized for each tissue. In fact, while standard extraction methods for other EVs are well described and include size exclusion chromatography, density gradient centrifugation and differential centrifugation, MBVs require tougher methods to be harvested. First, because MBVs are attached to the ECM, the ECM-derived material must first undergo a decellularization process to obtain dECM, which may include detergent-based and enzymatic decellularization methods. Secondly, the dECM must be solubilized to separate the MBVs from the collagen matrix. Once these steps are performed, MBVs can be isolated from the solubilized dECM using previously reported protocols for EVs [36] . This means that MBVs undergo several mechanical, chemical and enzymatic processes before the harvest, and each step can potentially change the characteristics, quality and performance of the resulting MBVs. Therefore, it is important to understand the presence, optimal collection method and role of MBVs in different dECM biomaterials to fully exploit the potential of these materials and apply them in regenerative contexts.

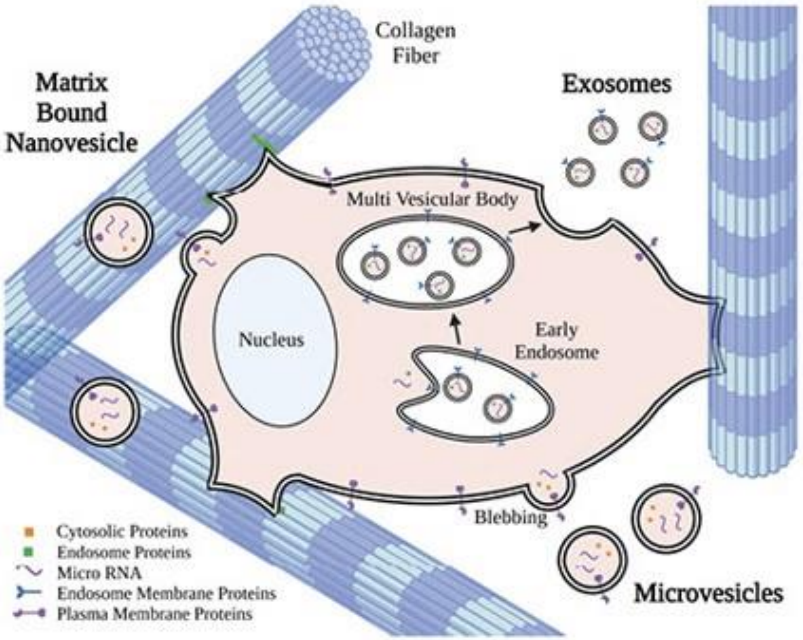

Figure 5 *Matrix-Bound Nanovesicles (MBVs): this illustration shows various types of vesicles originating from cells, including exosomes (50-100nm), microvesicles (100-1,000nm) and apoptotic bodies (1-5µm). MBVs are a newly discovered type of extracellular vesicles adhered to the ECM (Piening et al; 2023)*

These nanovesicles, which are attached to the extracellular matrix, possess unique characteristics that make them promising candidates for various therapeutic applications. Their attachment to the extracellular matrix provides them with stability and protection, allowing for prolonged circulation in biological fluids. Their small size enables them to easily penetrate tissues and cross biological barriers, facilitating targeted delivery of therapeutic cargo such as proteins, nucleic acids, and drugs to specific cells or tissues. MBVs have been shown to contain important cargo molecules such as microRNA that have the potential to regulate gene expression in endothelial cells, promoting angiogenic processes, suggesting that MBVs may play a role in enhancing the formation of new blood vessels within the ECM bioscaffolds, which is essential for tissue regeneration and repair [37]. This cargo can also influence cellular functions and modulate various physiological pathways, significantly contributing to the immunomodulatory capabilities of dECM biomaterials [37]. Various studies have demonstrated that MBVs, even when sourced from different tissues, exhibit the ability to mimic the immunomodulatory and regenerative properties of dECM. MBVs have been found to affect macrophage activation and differentiation. When macrophages were exposed to MBVs isolated from ECM bioscaffolds, they exhibited changes in surface marker expression associated with different macrophage phenotypes. This suggests that MBVs within ECM bioscaffolds can modulate the phenotype of macrophages, potentially promoting an anti-inflammatory response and tissue remodeling. By utilizing MBVs, researchers can harness the potential of these vesicles to enhance

tissue repair and regeneration, promote wound healing, and modulate immune responses. The ability of MBVs to deliver specific cargo molecules to target cells or tissues holds great promise in regenerative medicine [38]. These nanovesicles could serve as a platform for the targeted delivery of gene therapeutics and drugs, offering a non-invasive and potentially more effective approach to treating various diseases and injuries. Overall, MBVs play a crucial role in regulating tissue-specific functions, promoting tissue remodeling, facilitating cell-to-cell communication, and contributing to tissue homeostasis.

Research on MBVs focuses on understanding their origin, function, isolation methods, cargo characterization, and effects on cells. Furthermore, studies are being conducted to explore the potential use of MBVs as a platform for targeted delivery of gene and drug therapeutics. MBVs have been found in the urinary bladder matrix (UBM), submucosa of the small intestine (SIS), dermis, brain, heart, muscle, ovary and pancreas [36], [37], [39]. MBVs in UBM and SIS play a significant role in gastrointestinal system communication and have distinct functions depending on their tissue of origin. For instance, MBVs in the urinary bladder matrix contain miR-21, which is involved in regulating the PTEN/Akt pathway, affecting cell proliferation and metabolism. In the SIS, MBVs are rich in IL-33 and other cytokines that promote an anti-inflammatory macrophage phenotype, aiding in gastrointestinal health and repair [40]. In the dermis, MBVs are involved in skin health and wound healing processes. Brain-derived MBVs are crucial for neural communication and may have implications in neurological disorders. Heart tissue MBVs contribute valuable data on vesicles involved in cardiac function and potential implications for cardiovascular health, these MBVs contain miRNAs associated with oxidative stress and cell signaling, which are crucial for cardiac function and may have potential implications for cardiovascular health. Muscle, ovary, and pancreas-derived MBVs also exhibit tissue-specific functions, including roles in tissue regeneration, hormone regulation, and metabolic processes [36], [39], [41] . The protein concentration and particle yield of MBVs also differ by tissue, with UBM and SIS yielding higher concentrations of MBVs compared to other tissues. These differences underscore the importance of tissue-specific characteristics in MBV function and their potential applications in regenerative medicine and disease treatment.

By comprehensively studying the physical and compositional features of MBVs from different tissues, researchers can gain a deeper understanding of how these vesicles contribute to tissue-specific functions and regulatory mechanisms. This knowledge is essential for elucidating the roles of MBVs in maintaining tissue homeostasis, supporting tissue remodeling, and facilitating cellular communication within specific tissue environments.

3. OBJECTIVES

Recently research in regenerative medicine focused the attention on Matrix Bound Vesicles (MBVs) as potential contributors in maintaining and/or guiding cell behavior. The purpose of this study has been to evaluate the presence of MBVs in decellularized bovine pericardium (dBP), a well-known biological material that has been clinically applied in decellularization protocols and has shown excellent healing properties in various applications. MBVs, from dBP were characterized in terms of the tissue-specific physical and chemical properties, and their cytocompatibility was evaluated for regenerative medicine applications. Furthermore, preliminary studies on the immunomodulatory potential have been tested.

The use of different analytical techniques, including nanoparticle tracking assay (NTA) to determine the MBV size distribution, transmission electron microscopy (TEM) to provide valuable insights into their morphological features, and proteomic analysis to elucidate the protein and cytokine cargo encapsulated within these MBVs, have been performed.

In vitro experiments were performed using normal human dermal fibroblast cells (NHDFs) and human monocytes. Cytocompatibility was assessed by 3-(4,5-dimethylthiazol-2-yl)-2,5-dyphenyltetrazolium bromide (MTT) assay on NHDF and MBVs' effect on cell morphology was evaluated using phalloidin-DAPI immunofluorescence staining, while cytocompatibility was assessed by 3-(4,5-dimethylthiazol-2-yl)-5-(3-carboxymethoxyphenyl)-2-(4-sulfophenyl)-2H-tetrazolium (MTS) on human monocytes.

Concerning the protein content characterization, proteins were extracted from MBVs according to an adaptation of Subedi et al.'s method [42] and a silver staining after electrophoretic run was performed. Furthermore, a cytokine antibody array was used to detect the presence of cytokines in the protein extracts. The array, consisting of capture antibodies spotted on a membrane, allowed for the evaluation of 30 different cytokines. Finally, protein mass spectrometry was used for a comprehensive analysis of the protein composition. MBV samples were subjected to liquid chromatography with tandem mass spectrometry (LC-MS/MS) after protein extraction, precipitation, reduction, alkylation, and digestion. The acquired mass spectra were processed using data-independent mode (DIA) analysis, enabling the identification of proteins present in the samples.

Moreover, The MBVs'potential to drive M2 phenotype polarization was evaluated by M2 phenotype markers expression on cultured monocytes, by means of Real Time retro-transcriptase quantitative Polymerase Chain Reaction (real time-RT-qPCR).

The outcomes of the MTT viability assay showed no cytotoxic effects even at the highest concentration (9×10^7 MBVs/mL), while the lowest concentration of MBVs ($1{,}8 \times 10^7$ MBVs/mL) showed no enhancement with respect to cell viability, hypothesizing that MBVs at adequate concentrations allow and enhance cell viability. The findings of MBVs cytocompatibility were also confirmed by immunofluorescence analysis, as no cellular toxicity or significant changes in cellular morphology were seen. Similarly, MBVs increased cell viability in cultured human monocytes.

4. MATERIALS AND METHODS

4.1 Matrix-Bound Nanovesicles Isolation

Decellularized bovine pericardium extracellular matrix (dBP) was provided by Tissuegraft Srl. The dBP was freeze-dried and ground to a uniform powder. To extract the MBVs, dBP powder has been enzymatically digested [10 mg dry dBP/mL] by suspending it in a solution of collagenase type I [0.1 mg/mL] prepared in Tris-HCL [50 Mm, pH 7.4], NaCl [200mM], and $CaCl_2$ [5 mM] buffer. Enzymatic digestion in collagenase type I was performed for 24 h at 37°C in continuous rotation. The digested dBP was centrifuged at 100 × g for 5 min to remove residual matrix. The supernatant was collected and centrifuged at 10,000 × g for 90 min at 4°C. After, the supernatant was collected and ultracentrifuged at 100000 × g for 70 min at 4°C (Optima™ LE-80K ultracentrifuge, Beckman Coulter, Brea, CA, USA). The supernatant was discarded and the remaining pellet containing MBVs was resuspended in particle-free PBS [100 mg dry weight dBP/mL] and filtered with a 0.22 μm pore filter (Sartorius, 17823-K, Bohemia, NY, USA). Samples diluted in PBS were stored at -20° C until further use.

4.2 Nanoparticle Tracking Analysis (NTA)

dBP MBVs' size and concentration were determined by nanoparticle tracking assay (NTA). It provides information related to the size and concentration of nanoparticles in the sample. MBVs were resuspended in particle-free PBS and analyzed using a NanoSight N300 instrument (Malvern Panalytical, Malvern, UK). The size range of MBVs was determined by measuring the speed of Brownian motion which causes them to move randomly within the fluid. The camera captures the movement of these particles in real-time in three video recordings. MBV size was expressed as the mode ± standard error (SE) of the distribution, while MBVs concentration was indicated as the mean MBVs/mL ± SE.

4.3 Transmission Electron Microscopy (TEM)

MBV sample droplets (approximately 1.9 × 108 MBVs/mL) were placed on carbon-coated grids for 10 min and then fixed in 4% formaldehyde for 30 min. Grids were washed in distilled water, dried, and postfixed in 4% osmium tetroxide for 10 min at room temperature, after which the grids were washed in distilled water and stained with 2% uranyl acetate for 10 min at room temperature. After grids were dried, images were acquired at 120 kV using a Talos L120C G2 Transmission electron microscope (Thermo Fisher Scientific, Waltham, MA, USA) which provides detailed information about the structure and properties of materials at the nanoscale level.

4.4 Protein Content Characterization

4.4.1 Protein Extraction and Quantification

The method of Subedi et al. [42] was used to extract proteins from MBVs. Briefly, samples were lysed in a RIPA buffer for 30 min on ice and then mechanically dissociated using a GentleMACS ™ dissociator (Miltenyi Biotec, Gaithersburg, MD, USA). Protein concentration was measured using a bicinchoninic acid (BCA) protein assay kit (Novagen®, BCA Protein Assay Kit, 71285-3, Madison, WI, USA). As control, a hydrogel derived from enzymatic solubilization of dBP (dBP Gel) for both SDS-PAGE antibody and cytokine antibody array was used and lysed as previously described.

4.4.2 SDS-PAGE and Silver Staining

1 µg MBV protein extract was suspended in Laemmli sample buffer (Sigma-Aldrich, Milan, Italy) and placed in a 10% acrylamide solution (40%) was added (ITW Reagents, A4989, Monza, Italy). Electrophoresis was performed using a Mini-PROTEAN® electrophoresis module (Bio-Rad, Hercules, CA, USA) at 100 mV in a running buffer containing 0.1% SDS, 25 mM Trizma® base (Sigma-Aldrich, T1503, Milan, Italy). and192 mM glycine. After SDS-PAGE, silver staining was performed using the Pierce™Silver Stain Kit (Thermo Fisher Scientific, Milan, Italy) according to the manufacturer's protocol. Images were acquired using a ChemiDoc transilluminator (Bio-Rad, Hercules, CA, USA). The experiment was performed in triplicate.

4.4.3 Cytokine Antibody Array

To assess the presence of different cytokines in MBV protein extracts, a bovine cytokine array (RayBiotech, AAB-CYT-1, Peachtree Corners, GA, USA) was used according to the manufacturer's instructions. Briefly, the capture antibodies were released on a membrane and each pair of spots showing a different analyte, and these are as follows: aFGF (FGF-1), angiopoietin-1, bFGF, CD40 ligand (TNFSF5)), Decorin, GASP -1 (WFIKKNRP), IFN-alpha, IFN-beta, IFN-gamma, IGF-1, IL-1 alpha (IL-1 F1), IL-1 beta (IL-1 F2), IL-36 day (IL -1) F5), IL-10, IL-13, IL-15, IL-17A, IL-18, IL-2, IL-21, IL-4, IP-10(CXCL10), LIF, MCP-1 (CCL2) , MIG (CXCL9), MIP-1 beta (CCL4), NCAM-1 (CD56), RANTES (CCL5), TNF-alpha and VEGF-A. The sequence of the membrane sites is shown in Table 2. A total of 50 µg/mL of sample was used according to the manufacturer's protocol. Membranes were then imaged on a ChemiDoc (Bio-Rad, Hercules, CA, USA) for chemiluminescence detection and the experiment was performed in triplicate.

4.4.4 Protein Mass Spectrometry

MBV samples were frozen at −80°C immediately after separation for liquid chromatography with tandem mass spectrometry (LC-MS/MS). Samples were dissolved in RIPA buffer and sonicated. The proteins were then precipitated with cold acetone and resuspended. Proteins were reduced in 25 µl of 100 mM NH4HCO3 with 2.5 µl of 200 mM DTT (Merck, Milan, Italy) for 45 min at 60 °C and alkylated with 10 µl 200 mM iodoacetamide (Merck, Milan, Italy) within 1 hour at room temperature in the dark. Excess iodoacetamide was removed by adding 200 mM DTT. Samples were dried via Speed Vacuum and then desalted [43]. Digested peptides were analyzed on a nano Ultimate 3000 RSLC coupled directly to an Orbitrap Exploris 480 using a high-field asymmetric waveform ion mobility spectrometry (FAIMSpro) system (Thermo Fisher Scientific, Milan, Italy). Samples were inoculated into a C18 reverse phase (15 cm × 75 µm i.d., Thermo Fisher Scientific, Milan, Italy) and eluted with a gradient from 6% to 95% mobile phase B over 40 min using a flow rate of 500 mL/min, followed by equilibration with 6% mobile phase B for 1 min. The acquisition was performed in data-independent mode (DIA): precursor mass range was set between 400 and 900, isolation window of 8 m/z, window overlap of 1 m/z, HCD collision energy of 27%, orbitrap resolution of 30,000, and RF Lens at 50%. The normalized AGC target was set to 1000, the maximum injection time was 25 ms, and the microscan was 1. For DIA data processing, DIA-NN (version 1.8.1) was used: the identification was performed with “library-free search” and “deep learning-based spectra, RTs and IMs prediction” enabled. The enzyme was set to Trypsin/P; precursors of charge state 1–4, peptide lengths 7–30, and precursor m/z 400–900 were considered with a maximum of two missed cleavages. Carbamidomethylation on C was set as fixed modification and Oxidation on M was set as variable modification, using a maximum of two variable modifications per peptide. FDR was set to 1%.

Table 1 *The order of the cytokine spots on the Bovine Cytokine Array.*

POS	POS	NEG	NEG	aFGF	Angiopoietin-1	bFGF	CD40 Ligand (TNFSF5)	Decorin	GASP-1 (WFIKKNRP)	IFN alpha	IFN beta
POS	POS	NEG	NEG	aFGF	Angiopoietin-1	bFGF	CD40 Ligand (TNFSF5)	Decorin	GASP-1 (WFIKKNRP)	IFN alpha	IFN beta
IFN-gamma	IGF-1	IL-1 alpha (IL-1 F1)	IL-1 beta (IL-1 F2)	IL-36 Ra (IL-1 F5)	IL-10	IL-13	IL-15	IL-17A	IL-18	IL-2	IL-21
IFN-gamma	IGF-1	IL-1 alpha (IL-1 F1)	IL-1 beta (IL-1 F2)	IL-36 Ra (IL-1 F5)	IL-10	IL-13	IL-15	IL-17A	IL-18	IL-2	IL-21
IL-4	IP-10 (CXCL10)	LIF	MCP-1 (CCL2)	MIG (CXCL9)	MIP-1 beta (CCL4)	NCAM-1 (CD56)	RANTES (CCL5)	TNF alpha	VEGF-A	BLANK	POS
IL-4	IP-10 (CXCL10)	LIF	MCP-1 (CCL2)	MIG (CXCL9)	MIP-1 beta (CCL4)	NCAM-1 (CD56)	RANTES (CCL5)	TNF alpha	VEGF-A	BLANK	POS

4.5 Cytocompatibility

4.5.1 Cell Culture

Normal human dermal fibroblast cells (NHDFs) (Lonza NHDF-Ad CC-2511, Basel, Switzerland) were used for cell viability assay and immunofluorescence. Cells were cultured in 75 cm2 flasks, maintained in Dulbecco's Modified Eagle Medium (DMEM) (Gibco 21068-028, Milan, Italy), supplemented with 5 mM glutamine (Sigma-Aldrich 1294808, Milan, Italy), 1% penicillin, streptomycin and amphotericin-B (PSF) (Euroclone, Milan, Italy), and 10% foetal bovine serum (FBS) (Gibco, Milan, Italy). Cells were used up to the 6th passage.

Human monocytes were isolated from buffy coat of healthy donors, with use of the Histopaque protocol (Sigma Aldrich, Histopaque®-1077, Italy). The maintenance media used is Rosewell Park Memorial Institute (RPMI) 1640 (Lonza, Switzerland), decomplemented FBS was used at either 20% or 10% depending on experiment conditions. Cells were used for the evaluation of cell viability and immunomodulatory potential from the buffy coat. In order to induce M0, RPMI 20% FBS was used. To induce M1, RPMI 10% FBS plus GM-CSF was used, and to induce M2, RPMI 10% plus M-CSF was used. Moreover, different cytokines were used to direct the differentiation towards M1 or M2, specifically, interferon-gamma (INF) was added in a ratio 1:5000, lipopolysaccharide (LPS) in a ratio 1:100, and interleukin-4 (IL-4), interleukin-10 (IL-10), and interleukin-13 (IL-13) in a ratio 1:5000.

4.5.2 Cell Viability

MBVs were tested for cytocompatibility using the MTT assay (MerckMillipore, Darmstadt, Germany). Cells were seeded in 48-well plates at a concentration of 8000 cells/well. After 24 hours, the culture medium was replaced with a medium containing MBVs, precisely, MBVs previously diluted in PBS at various concentrations: 9×10^7 MBV/mL, 3.6×10^7 MBV/mL, and 1.8×10^7 MBV/mL. A total of 500 µl of PBS containing MBV was added to each well, along with 500 µl of culture medium. To have a control, medium/PBS was used in a ratio of 1:1. For a positive control of cell death, 2.5% dimethyl sulfoxide (DMSO, Sigma-Aldrich, Milan, Italy) was used. At 1 and 3 days after the addition of MBVs into the cells, MTT assay was performed by discarding culture media and adding DMEM 10% FBS supplemented with 0.5 mg/mL MTT (Sigma- Aldrich, Italy). After 4 h, media were discarded and 100 µl of DMSO was added. The 570 nm absorbance was read using Victor4X Multilabel Plate Reader (Perkin Elmer, Milan, Italy) and data were analyzed in Excel (Microsoft, Redmond, WA, USA). Experiments were performed in triplicate.

Human monocytes were tested for cytocompatibility using the MTS assay (Promega, Madison, USA). Human monocytes isolated from buffy coat were directly seeded in 96-well plates at a concentration of 100.000 cells per well. MBVs were added at a concentration of 0.5×10^{15}, and the cells were maintained in RPMI 20% FBS. On day 7 MTS assay was performed.

4.5.3 Immunofluorescence

Phalloidin-DAPI immunofluorescence staining was used to evaluate MBVs' effect on NHDF cell morphology. Cells were seeded in 24-well plates over microscope glass slides, at a concentration of 14000 cells/well. After 24 h, the culture medium was replaced with MBV-containing medium; specifically, MBVs previously diluted in PBS at different concentrations of 9 × 107 MBVs/mL, 3.6 × 107 MBVs/mL, and 1.8 × 107 MBVs/mL. A total of 750 µL of PBS containing MBVs was placed in each well, and 750 µL of culture medium was added. In order to obtain representative control, a medium/PBS in a ratio of 1:1 was used. At time points of 1 and 3 days after MBVs were added to cells, samples were fixed using 4% formaldehyde for 1h at room temperature. Phalloidin, Fluorescein Isothiocyanate Labeled (Sigma-Aldrich, P5282, Milan, Italy) was placed over the samples and incubated at 37 ◦C for 45 min. Nuclei were stained with 1 µg/mL DAPI (Sigma-Aldrich, Milan, Italy) for 1 min. Stained cells were observed using a fluorescence microscope (Leica DM700, Wetzlar, Germany), and images were acquired via Leica software LAS V4.7 (Leica, Wetzlar, Germany). Experiments were performed in triplicate.

4.6 Macrophages cytocompatibility and monocytes polarization

Real time-RT-qPCR was used to access the expression of M1 and M2 macrophage phenotype markers of human monocytes. Human monocytes were used at a concentration of 500.000 cells per well. MBVs at a concentration of 0.5×10^{15} were added. After 6 days, cytokines were added to boost the macrophage polarization.

On the 7th day, RNA was extracted: cell monolayer was rinsed with PBS, lysed in 500 µL of TRIzol (Thermo Fisher Scientific, Italy) for 5 minutes, and mechanically detached using a scraper. Samples were collected in 2 mL tubes and stored at -80° C until RNA purification, performed with 100 µL of chloroform (Sigma Aldrich, Italy) and 12 000 rpm centrifugation for 15 minutes at 4° C according to manufacturer's protocol. The aqueous phase containing RNA was transferred to a clean tube and 250 µL of isopropanol 20 (Sigma Aldrich, Italy) were added, after 12000 x g centrifuge for 15 minutes at 4° C RNA pelleted at the bottom and isopropanol was discarded and replaced with 500 µL of ethanol 75% (Sigma Aldrich, Italy), quantified spectrophotometrically with Nanodrop (Thermo Fisher Scientific, Italy) by measuring the optical density at 260 and 280 nm and stored until retro-transcription. Retro-transcription was performed according to High-Capacity RNA-to-cDNA™ Kit

(Applied Biosystems, USA) manufacturer instructions. cDNA obtained was stored at -20° C until further use. Real-time quantitative PCR was performed in 10 µL volumes, 9 µL of PCR mix and 1 µL of sample. PCR mix was prepared according to SsoAdvanced Universal SYBR Green Supermix (BioRad, USA) protocol with 4% 0.1mM forward and reverse primers for CD80 and CD86, CD163 and CD206, TNF-α and Glyceraldehyde 3-phosphate dehydrogenase (GADPH) used for normalization.

5. RESULTS

5.1 Matrix-Bound Nanovesicles from Decellularized Bovine Pericardium Morphological Characterization

Nanoparticle tracking analysis (NTA) and transmission electron microscopy (TEM) showed the presence of nanovesicles isolated from dBP by enzymatic isolation and differential centrifugation. NTA was performed on MBVs resuspended in particle-free phosphate-buffered saline (PBS) and showed that an average of $1.9 \times 10^8 \pm 0.22 \times 10$ MBV/ml could be obtained starting with 100 mg dry weight dBP. The mode size of the MBVs was 142 ± 1.5 nm. **Fig. 6A** shows a representative curve of one NTA analysis of a triplicate sample showing a peak in MBV size between 100 and 200 nm, which correlates with the size of MBVs found in the literature. The size range of MBVs was also confirmed by TEM analysis [**Fig. 6B**], which found MBVs characterized by a generally circular lipidic membrane stained in black with osmium tetroxide. Some MBVs were observed aggregated with each other. In addition, most MBVs showed additional globular lipid structures within the vesicles.

A

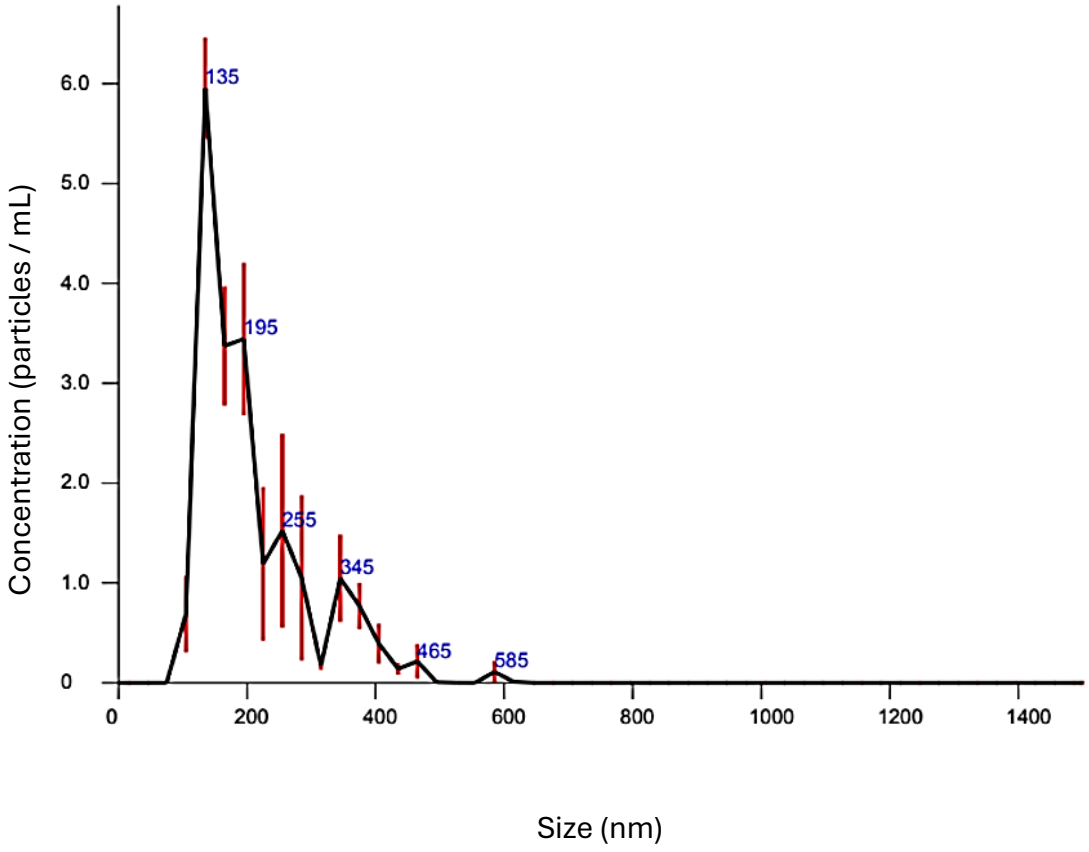

B

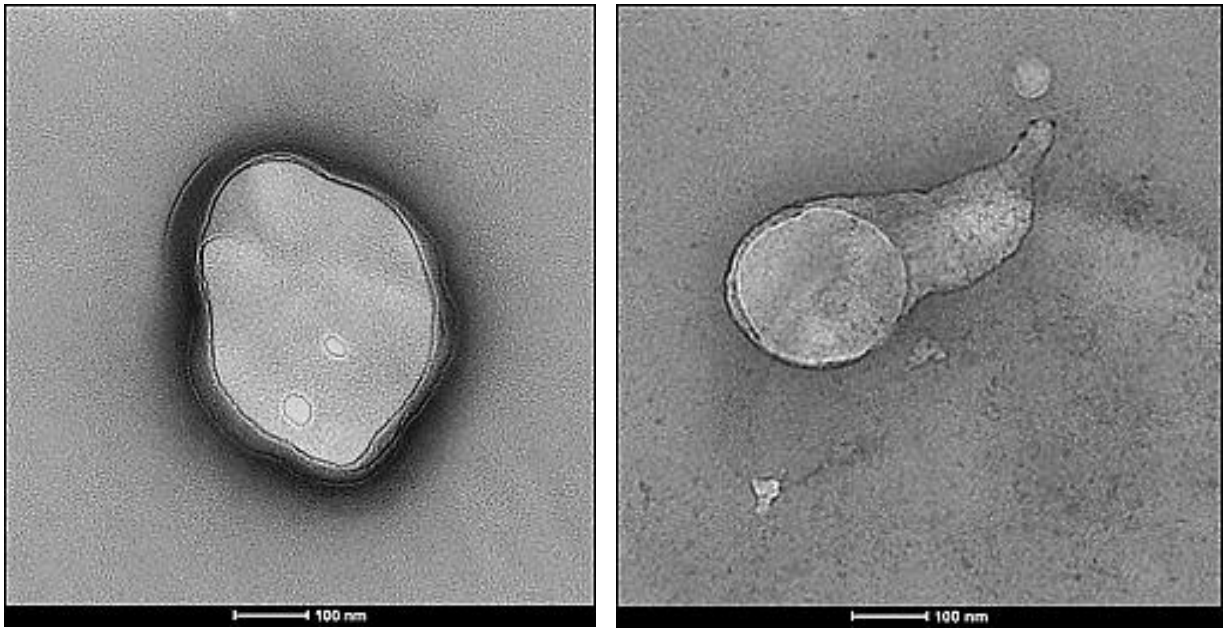

Figure 6 (A) *Representative concentration-size distribution of NTA analysis on MBVs. Red bars indicate ± standard error of the mean.* ***(B)****: Representative of TEM images of MBVs fixed on carbon-coated grids. Scale bar 100nm.*

5.2 Matrix-Bound Nanovesicles Chemical Characterization

5.2.1 SDS-Page and Silver Staining

Silver staining was performed on MBV proteins isolated from different batches of bovine pericardium (MBV.1 and MBV.2) and proteins extracted from a dBP gel; a representative image of the experimental triplicate samples is shown in **Fig. 7** The dBP gel was obtained by a dBP solubilization process that preserved the protein content of the original DBP matrix containing MBVs, while only protein-containing nanovesicles should be retained when MBVs were extracted. The results show different protein profiles, and in both conditions (dBP gel and MBVs), different proteins such as 135 kDa, ~70 kDa and ~48 kDa were significantly more expressed in MBV samples. In addition, the protein profiles of MBV.1 and MBV.2 were comparable.

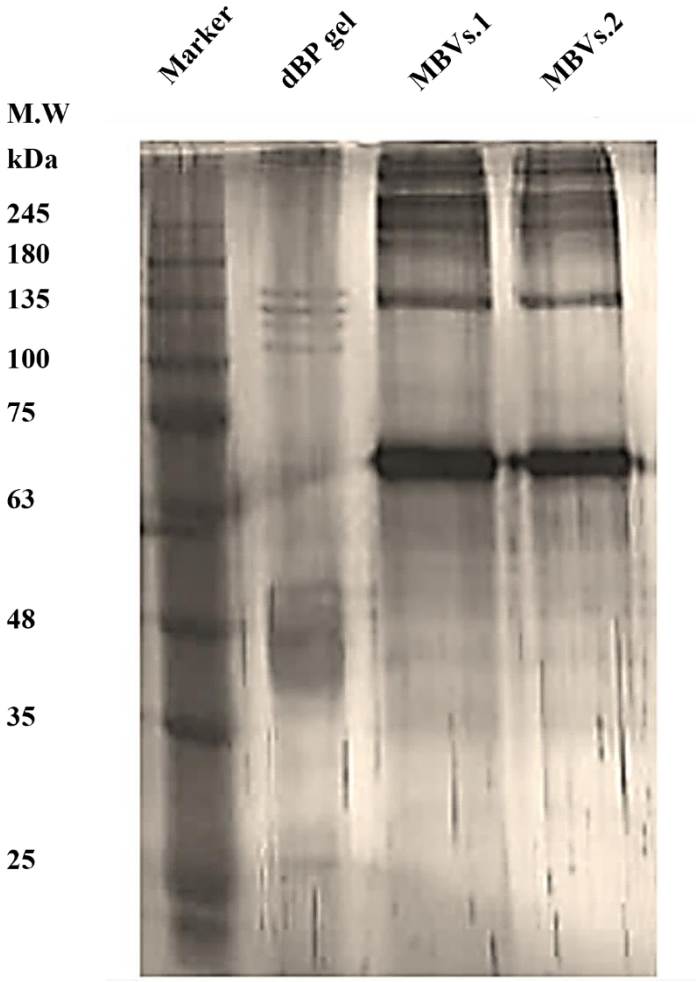

Figure 7 *Silver Stain on SDS-Page. Samples were loaded as follows, left to right: protein marker, dBP gel, MBV.1, MBV.2.*

5.2.2 Cytokine Antibody Array

Cytokine analysis results revealed different cytokines and chemokines contained in MBVs. The detected molecules had visible spots on the array membranes, the density of which correlated with the amount of the observed molecule. **Fig. 8A** shows representative membrane images (from experimental triplicates) of cytokine concentration in dBP gel and MBVs. Twenty different cytokines were highlighted in the samples [**Fig. 8B**]; especially acidic and basic fibroblast growth factors (aFGF and bFGF), interferon (IFN) gamma, interleukin (IL) 1 alpha, 10, 15, IL-21, IFN gamma-induced protein 10 (IP-10), neural cell adhesion molecule (NCAM) 1 and tumor necrosis factor (TNF) alpha were found in higher amounts in MBVs (pink in Figure 8B), while decorin, IFN-alpha and beta, insulin-like growth factor (IGF) 1, leukemia inhibitory factor (LIF), monocyte chemoattractant protein (MCP) 1, monokine induced by IFN-gamma (MIG), macrophage inflammatory protein (MIP) 1 beta, and chemokine ligand 5 (RANTES) were found were found to be expressed in both MBV and dBP gel samples (orange in Figure 8B). Finally, only vascular endothelial growth factor (VEGF) A and not in MBVs. (violet in Figure 8B).

5.2.3 Protein Mass Spectrometry

The mass spectrometry results revealed the protein profiles of MBVs extracted from two distinct pericardium batches, labeled as MBV.1 and MBV.2. In Table 1, the proteins identified in both batches are listed, with 45 proteins detected in MBV.1 and 23 in MBV.2. Among these, 18 proteins were common to both batches, including collagen type I, albumin, vimentin, annexin A2, heat shock protein 70 kDa 1-like, complement component C6, tubulin, actin, asporin, histone H4, and prolargin. Additionally, glycoproteins (such as fibulin-5, fibrillin, fibronectin, and alpha-2-HS-glycoprotein) and proteoglycans (including mimecan and decorin) were also identified [**Table 2**].

A

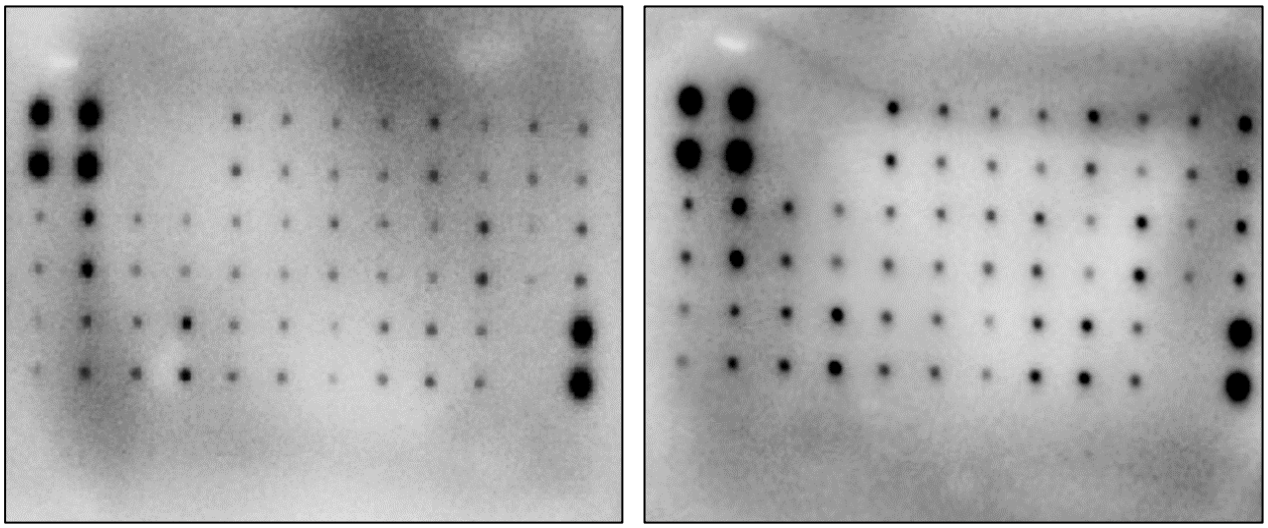

B

POS	POS	NEG	NEG	aFGF	Angiopoietin-1	bFGF	CD40 Ligand (TNFSF5)	Decorin	GASP-1 (WFIKKNRP)	IFN-α	IFN-β
POS	POS	NEG	NEG	aFGF	Angiopoietin-1	bFGF	CD40 Ligand (tTNFSF)	Decorin	GASP-1 (WFIKKNRP)	IFN-α	IFN-β
IFN-γ	IGF-1	IL-1α (IL-1F1)	IL-1β (IL-1F2)	IL-36 Ra (IL-1 F5)	IL-10	IL-13	IL-15	IL-17A	IL-18	IL-2	IL-21
IFN-γ	IGF-1	IL-1α (IL-1F1)	IL-1β (IL-1F2)	IL-36 Ra (IL-1 F5)	IL-10	IL-13	IL-15	IL-17A	IL-18	IL-2	IL-21
IL-4	IP-10 (CXCL10)	LIF	MCP-1 (CCL2)	MIG (CXCL9)	MIP-1β (CCL4)	NCAM-1 (CD556)	RANTES (CCL5)	TNFα	VEGF-A	BLANK	POS
IL-4	IP-10 (CXCL10)	LIF	MCP-1 (CCL2)	MIG (CXCL9)	MIP-1β (CCL4)	NCAM-1 (CD556)	RANTES (CCL5)	TNFα	VEGF-A	BLANK	POS

Figure 8 (A): *Representative antibody array membrane of dBP gel and MBV samples of experimental triplicates using different MBV batches.* ***(B):*** *Table showing the order of the cytokine spots on the antibody array membrane. Highlighted in orange are cytokines found to be expressed in both dBP gel and MBVs; in violet, cytokines expressed in gel dBP only; in pink, cytokines expressed in MBVs only; and in grey the cytokines that were not expressed in any of the samples.*

Table 2 *Proteins found in MBV.1 and MBV.2 from LC-MS/MS. ✓: proteins represented in the MBV batch.*

Protein	MBV.1	MBV.2
Total	**45**	**23**
Transthyretin	✓	
Keratocan	✓	
Prothrombin	✓	
Protein AMBP	✓	
Collagen alpha-1(I) chain	✓	✓
Collagen alpha-2(I) chain	✓	✓
Fibrinogen beta chain	✓	
Albumin	✓	✓
Annexin A2	✓	✓
Fibronectin	✓	✓
Heat shock 70kDa protein 1-like	✓	✓
Galectin-1	✓	
Alpha-2-HS-glycoprotein	✓	✓
Apolipoprotein A-I	✓	
Mimecan	✓	✓
Decorin	✓	✓
Protein-lysine 6-oxidase	✓	
Alpha-1-antiproteinase	✓	
Vimentin	✓	✓
Transforming growth factor-beta-induced protein	✓	
Actin	✓	✓
Ras-related protein Rap-1b	✓	
Histone H4	✓	✓

Protein	MBV.1	MBV.2
Total	**45**	**23**
14-3-3 protein zeta/delta	✓	
Elongation factor 1-alpha 1	✓	
Tubulin alpha-4A chain	✓	
Fibrillin-1	✓	✓
Endoplasmic reticulum chaperone BiP	✓	
Myosin-10	✓	
Latent-transforming growth factor beta-binding protein 2	✓	
Complement component C6	✓	✓
Tubulin beta-5 chain	✓	✓
Complement C3	✓	
Thrombospondin-4	✓	
Gelsolin	✓	
Heat shock protein beta-1	✓	
Asporin	✓	✓
Fibulin-5	✓	✓
Tropomyosin alpha-3 chain	✓	
Small ribosomal subunit protein eS12	✓	
Heat shock protein HSP 90-beta	✓	
Alpha-2-macroglobulin	✓	
Juncton plakoglobin		
Prolargin	✓	✓
Myocilin	✓	
Collagen alpha-1(III) chain		✓
LIM and SH3 domain protein 1		✓
Fibrinogen gamma-B chain		✓
Cadherin-13		✓

5.3 Matrix Bound Nanovesicles Cytocompatibility

To evaluate the cytocompatibility of MBVs with normal human dermal fibroblast (NHDF) cells at different concentrations, Thiazolyl Blue Tetrazolium Bromide (MTT) viability assay and phalloidin-4′,6-diamidino-2-phenylindole (DAPI) immunofluorescence staining were performed. **Fig. 9A** shows the viability assay, demonstrating no statistical differences between the control (CTR) and cells treated with different concentrations of MBVs on day 1. While the control showed no significant increase from day 1 to day 3, cells treated with concentrations of 9×10^7 MBVs/mL and 3.6×10^7 MBVs/mL showed a statistically significant increase in cell viability from 1 and day 3. Interestingly, these MBV-treated conditions exhibited significantly higher cell viability on day 3 compared to the respective control, whereas the 1.8×10^7 MBVs/mL condition, while not inducing cell toxicity, did not enhance cell viability. Dimethyl sulfoxide (DMSO) was used as a control for cell death, revealing statistically significant decreases in cell viability on both days 1 and 3 compared to cell viability across all other conditions. These findings were confirmed by immunofluorescence analysis [**Fig. 9B**], where cell morphology assessed through phalloidin-DAPI staining was comparable between MBV groups and the control. In summary, MBVs at different concentrations did not show cell toxicity or induce alterations in NHDF cell morphology after 3 days of treatment.

With respect to human monocytes, MBVs showed an optimal cytocompatibility significantly increasing cell viability from day 1 to day 7. [**Fig. 9C**].

A

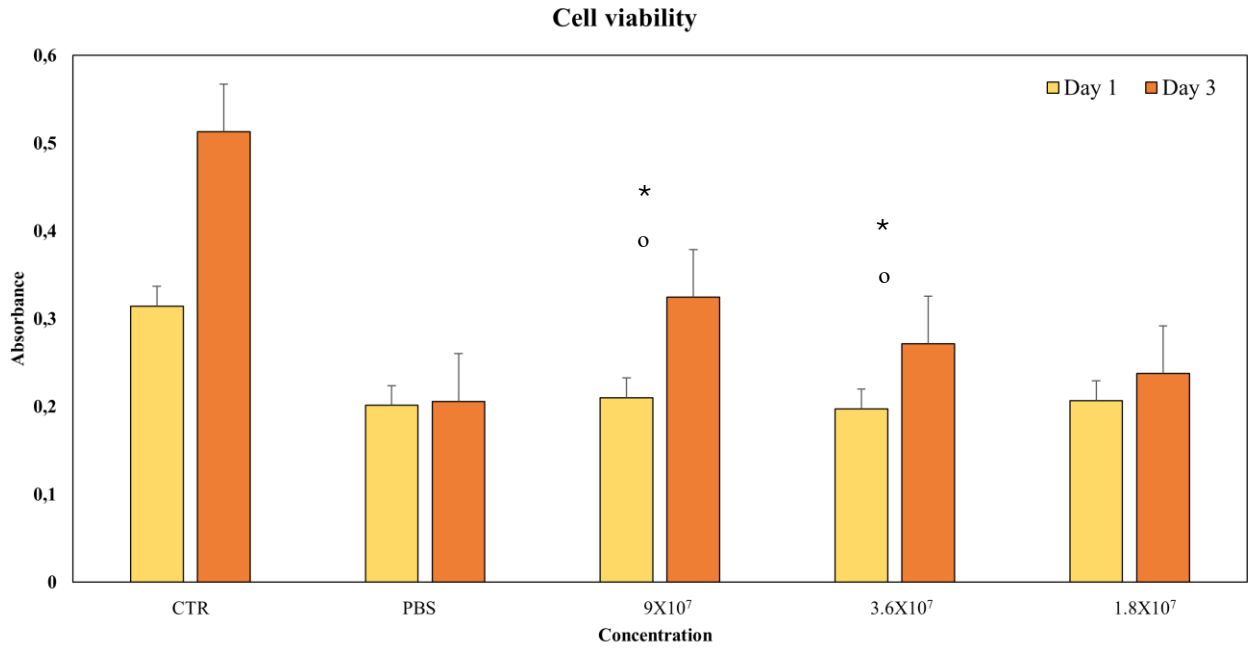

B

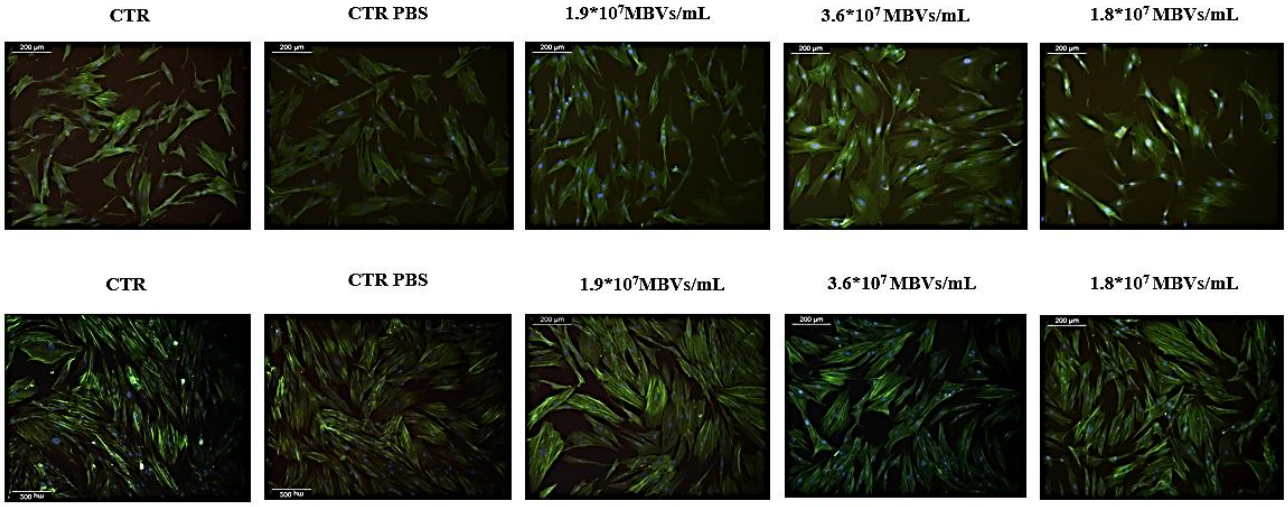

C

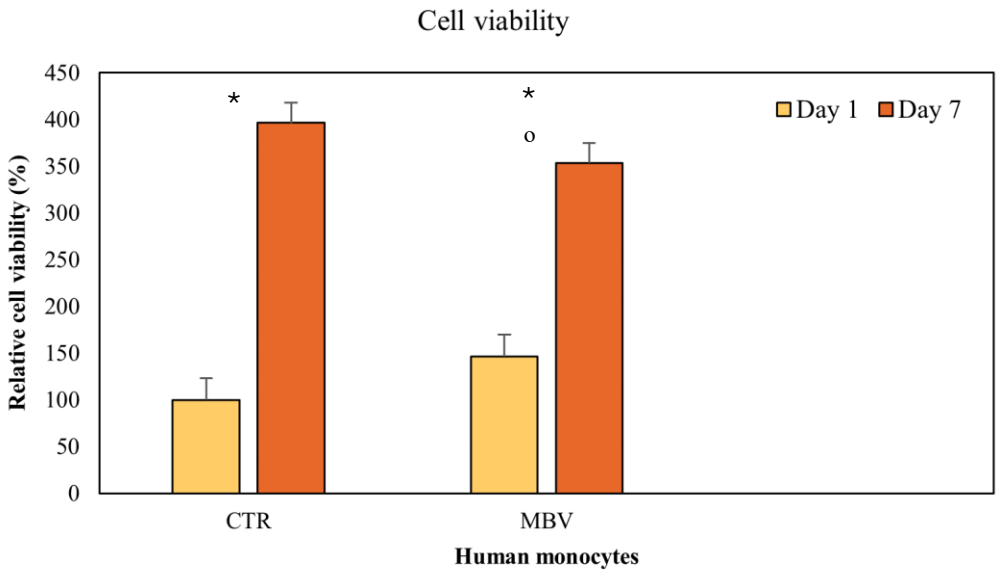

***Figure 9 (A)**: MTT viability assay on NHDF cells treated with different concentrations of MBVs for 1 and 3 days. Data are indicated as mean ± S.D. of triplicate. *: day 1 vs. day 3; °: MBV vs. CTR day 3; ^: DMSO vs. all conditions, p< 0.05. **(B)**: Phalloidin-DAPI immunofluorescence staining on NHDF cells treated with different concentrations of MBVs for day1 and 3 days. Images are representative of experimental triplicates. **(C):** MTS viability assay on human monocytes treated with MBVs. Data are indicated as mean ± S.D. of triplicate. *: day 1 vs day 7; p < 0.005 °.*

5.4 Matrix Bound Nanovesicles Immunomodulatory potential

The macrophage phenotype was evaluated using typical M1 and M2 markers expressed. In particular, Real time-RT-qPCR was used to assess the expression of M2 phenotype markers CD163 and CD206, **[Fig.10]**, of M1 phenotype markers TNF-α, CD80 and CD86 **[Fig.11].** As shown by the graphs, although these results are preliminary due to a limited repeated experiments and the consequent lack of statistical significance. M0 macrophages in presence of MBVs do not show any changes with respect to M0 control. However, when induced towards an M1 response, despite the increase of inflammatory markers, M2 are enhanced as well.

In the case of M2 differentiation, there is an increased expression of the anti-inflammatory marker compared to the control.

These preliminary findings suggest that MBVs do not alter the macrophage behavior, while enhancing M2 polarization also when environmental conditions are mimicking the inflammatory conditions. Further extensive experiments are needed to confirm these observations and to explore the underlying mechanisms.

A

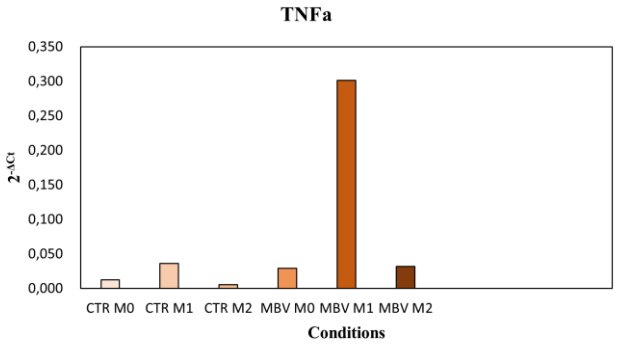

B

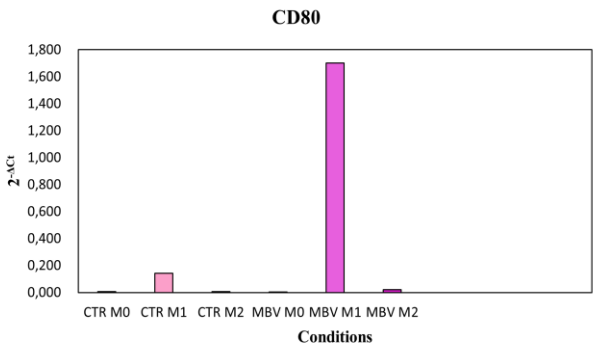

C

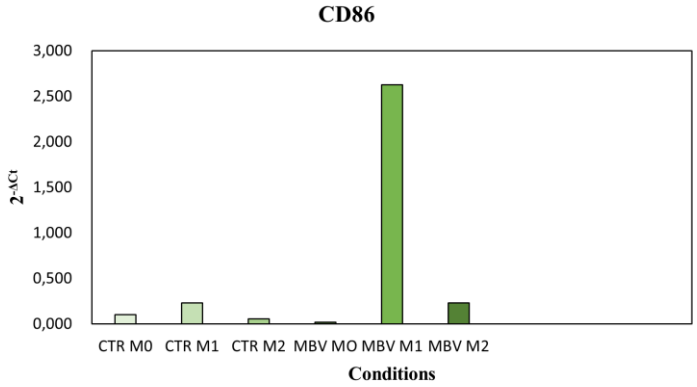

Figure 10 *Real time-RT-qPCR for expression of M1 phenotype markers by human monocytes.* ***(A):*** *Shows the expression of the M1 phenotype marker TN-α.* ***(B):*** *Shows the expression of the M1 phenotype marker CD80.* ***(C):*** *Shows the expression of the M1 phenotype marker CD86.*

A

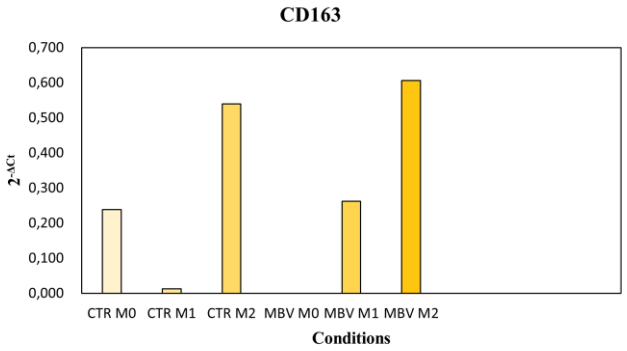

B

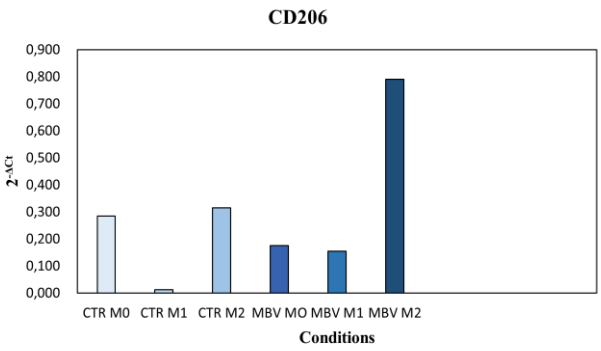

Figure 11 *Real time-RT-qPCR for expression of M2 phenotype markers by human monocytes.* ***(A):*** *Shows the expression of the M2 phenotype marker CD163.* ***(B):*** *Shows the expression of the M2 phenotype marker CD206.*

6. DISCUSSION

In this study, the presence of matrix-bound nanovesicles (MBVs) in decellularized bovine pericardium (dBP), their physical and chemical properties, as well as cytocompatibility were evaluated. Through analyses employing nanoparticle tracking analysis (NTA) and transmission electron microscopy (TEM), nanovesicles ranging from 100 to 200 nm, characterized by lipidic membranes, were successfully isolated from dBP. These findings corroborate the existence of MBVs within dBP, a subclass of extracellular vesicles (EVs), thus delineating a distinct population adhering to the extracellular matrix (ECM), contrary to conventional EVs presumed to exist solely within bodily fluids [36].

The observed size range and structural features of MBVs align with previous reports in the literature, thereby affirming their consistency across different tissue sources [39], [41], [44]. Notably, TEM images unveiled internal vesicular structures within MBVs, analogous to other EV subtypes [45]. Remarkably, the persistence of MBVs within decellularized tissues underscores their ability to remain bound to the collagen matrix post-decellularization, suggesting release only upon specific enzymatic degradation. The employed isolation methodology, integrating collagenase degradation and gradient centrifugation, yielded an average concentration of $1.9 \times 10^8 \pm 0.22 \times 10^8$ MBVs/mL from 100 mg of dry weight dBP [36], [41]. Although slightly lower than reported yields in the literature, these results reinforce the presence of MBVs in yet another decellularized tissue, underscoring both tissue-specific and method-dependent variations.

Nonetheless, our findings provide evidence for the existence of this newly identified subclass of extracellular vesicles (EVs) within yet another decellularized tissue. This discovery suggests the presence of an additional signaling mechanism not only within the extracellular matrix (ECM) but also in biomaterials derived from decellularized ECM. Importantly, these vesicles are only released following enzymatic degradation of the matrix and/or biomaterial, indicating a tightly regulated mechanism for their release [36], [46]. EVs are renowned for their potent cell signaling capabilities, and significant discoveries have been made regarding their pivotal paracrine roles. These roles include physiological and pathological processes, including but not limited to angiogenesis, immunomodulation, cell proliferation and differentiation, and tissue repair [16], [47].

Furthermore, this potential comes from the highly bioactive cargo carried by extracellular vesicles (EVs), which has been extensively studied for well-known EV types in recent years [36], [38], [39]. However, in the case of matrix-bound nanovesicles (MBVs), their recent discovery means that less is known about their cargo. While there has been more research focused on understanding the nucleic acid and lipidic content of MBVs, a thorough characterization of their protein content has yet to be

reported. This is particularly crucial because the cargo of MBVs is known to be tissue-specific and plays a significant role in conferring the bioactive properties to the source decellularized ECM (dECM) material. Therefore, unraveling the protein and cytokine content of MBVs is essential for comprehending their potential in cellular signaling the extensive characterization of MBV cargo. Silver staining of SDS-PAGE revealed a complex protein profile in MBVs, with comparative analyses against dBP gel, representing the parent dECM material, elucidating subtle differences in protein composition. Notably, cytokine assays unveiled a diverse array of bioactive molecules expressed in MBVs, encompassing growth factors, cytokines, and chemokines implicated in various physiological and pathological processes, including immunomodulation and tissue repair. When comparing the protein content of MBVs to the dBP gel, some distinctions become apparent. While the main bands observed in the MBV samples are also present in the dBP gel, albeit with lower expression, this discrepancy can be attributed to the presence of MBVs within the dBP gel. Despite this, the dBP gel exhibits a more diverse protein profile, enriched with dECM proteins retained within the sample. Nonetheless, MBVs show a substantial protein content that warrants further investigation. Furthermore, the cytokine assay results reveal a rich and bioactive repertoire of 19 different cytokines expressed in MBVs. Among these, 9 cytokines were expressed both in MBVs and the dBP gel, while 10 others appear to be exclusively expressed in MBVs. Notably, VEGF-A is expressed solely in the dBP gel. This different array of cytokines, chemokines, and growth factors underscores the immunomodulatory potential of MBVs, playing crucial roles in processes such as tissue repair and angiogenesis [47], [48]. Among the expressed growth factors and hormones, acidic and basic FGFs emerged, known for their involvement in tissue repair and angiogenesis, alongside IGF-1, recognized for its regulatory functions in cellular and metabolic processes, including anti-inflammatory effects [49], [50]. The presence of the proteoglycan decorin is also notable, given its pivotal role in ECM integrity and immunomodulation [50], [51]. Interferons alpha, beta, and gamma were expressed, which play pro-inflammatory, anti-inflammatory, and anti-viral roles [52], [53]. Other potent activators of the immune system were found, including TNF-alpha and a diversity of interleukins, like IL-1 alpha, IL-15, and IL-21, or immunosuppressive ones, such as IL-10 [52], [54], [55]. Different chemoattractant chemokines were expressed, like MIP-1 beta, MIG, RANTES, MCP-1, and IP-10 [56], [57]. Multifunctional glycoprotein NCAM-1 was also present, which plays a role in cell–cell interactions and cell–matrix interactions, immune system surveillance, and nervous system development [58], [59]. Overall, these findings further explain the cell-signalling properties and immunomodulatory potential of MBVs which were already described in the literature. Moreover, the tissue-specificity of the cytokine cargo was also confirmed.

Moreover, mass spectrometry elucidated the presence of 18 proteins shared across different MBV batches, predominantly comprising ECM-secreted proteins and cytoplasmic proteins. Noteworthy constituents such as collagen type I, which can be secreted in extracellular vesicles for cell-signalling between cells and elastic fibers proteins such as fibrillin-1, and fibronectin that underscored the involvement of MBVs in ECM-associated processes, suggesting a distinct biogenesis from other EV subtypes [60]. Mimecan, a well-known component of bovine tissues, was identified within MBVs, showcasing its growth factor activity and involvement in ECM assembly. Additionally, the presence of fibronectin, a protein implicated in various EV-cellular interactions [61], is noteworthy for its anti-fibrotic activity in tissue repair. Annexin 2, typically found in mineralizing tissues, was also detected, suggesting its role in EV protein trafficking [62]. Furthermore, the confirm of decorin underscores its significance in maintaining ECM integrity and modulating immune responses. Cellular cytoplasmic proteins such as vimentin, tubulin, actin, and histone H4 were also identified within MBVs. These proteins are known to be present extracellularly in vesicles [63], [64], suggesting a potential role for MBVs in mediating cell-matrix interactions and ECM remodeling. The prevalence of ECM-related proteins in MBVs indicates their secretion during ECM-involved processes, implying a distinct biogenesis from other EV subtypes. Interestingly, our analysis revealed differences in the protein composition between the two MBV batches. While the process of dBP decellularization is standardized, variations observed may come from inherent batch-to-batch differences in biomaterials sourced from animal origin [65], [66]. Notably, differences primarily manifested in the loss of cellular-related peptides, such as enzymes, while ECM-related proteins remained consistent. This suggests that the intrinsic bioactivity of MBVs is preserved across batches [65], [67], despite variations in protein composition. These findings not only shed light on the bioactive mechanisms underlying ECM-mediated paracrine signaling but also underscore the potential of dECM biomaterials in regenerative medicine. Our study demonstrates that dBP harbors signaling factors protected by lipidic membranes, tightly bound to the biomaterial matrix, and released upon enzymatic degradation. This knowledge is invaluable for designing biomaterials capable of harnessing and delivering immunomodulatory and regenerative molecules, paving the way for innovative applications in regenerative medicine [68], [69], [70].

Despite variations observed between MBV batches, attributed to inherent batch-to-batch disparities in biomaterials of animal origin, the preservation of intrinsic bioactivity underscores the potential of MBVs for therapeutic applications [65], [66].

The assessment of MBV cytocompatibility on normal human dermal fibroblasts (NHDFs) reaffirmed previous reports of non-cytotoxic effects of MBVs even at high concentrations of 10^{11} MBVs/mL [71]

however, lower concentrations able to produce a biological effect in terms of cellular viability were chosen. The outcomes of the MTT viability assay showed that even at the highest concentration (9×10^7 MBVs/mL) given to cells, no cytotoxic effects were seen. MBV concentrations of 9×10^7 MBVs/mL and 3.6×10^7 MBVs/mL induced a significant increase in cell viability from day 1 to day 3 of cell culture, while also displaying a higher cell viability at day 3 when compared to CTR. The lowest concentration of MBVs used showed no enhancement with respect to cell viability. Thus, we can speculate that MVBs at adequate concentrations allow and enhance cell viability through a richer milieu, as proved by the bioactive molecules found in their cargo. The findings of MBV cytocompatibility were also confirmed by immunofluorescence analysis, as no cellular toxicity or significant changes in cellular morphology were seen according to the literature [44], [71], [72]. Despite the comprehensive insights garnered, the study acknowledges certain limitations, emphasizing the need for further in-depth characterization, including surface marker profiling and analysis of lipidic and nucleic acid content, to fully unravel the biological potential of MBVs isolated from dBP. Nonetheless, the rich bioactivity exhibited by MBVs, coupled with their unique properties, portends promising avenues for regenerative medicine applications, warranting continued exploration into their therapeutic potential. MBVs, with their unique potential for immunomodulatory and regenerative medicine applications, offer a promising avenue for therapeutic development. Their ability to transfer bioactive components, coupled with their nanoscale nature, positions MBVs as a novel therapeutic tool in regenerative medicine.

Finally, although the results from the immunomodulation are preliminary due to the lack of statistical significance, it seemed that MBVs, when induced towards an M1 response, exhibited both an inflammatory and anti-inflammatory reaction. This suggests a transitional phase in the macrophage polarization response. In this phase, macrophages might be shifting from an inflammatory to an anti-inflammatory state, thus expressing both inflammatory and anti-inflammatory markers. Therefore, MBVs could be facilitating the transition of macrophages that were initially set to be inflammatory to become anti-inflammatory. As a result, these macrophages expressed markers characteristic of both states, indicating a transitional period.

Since these results are preliminary, extensive further experiments are required to confirm them and to understand their implications fully. The dual expression of markers suggested a complex interplay during macrophage polarization that needs to be elucidated through additional research. Understanding this transition could provide significant insights into the regulatory mechanisms of macrophage function and the potential therapeutic applications of MBVs in modulating immune responses.

In conclusion, our study identified and characterized matrix bound nanovesicles isolated from decellularized bovine pericardium ECM, corresponding to the newly described MBVs. These MBVs were found to harbor a rich and bioactive cargo, encompassing a tissue-specific array of proteins, cytokines, chemokines, and growth factors, reminiscent of the contents found in the parent dBP. Furthermore, MBVs demonstrated cytocompatibility and the ability to enhance cell viability. These findings lay the groundwork for future investigations into MBVs from dBP, exploring their potential in various aspects of regenerative medicine, including immunomodulation, angiogenesis, stem cell differentiation, and wound healing.

7. REFERENCES

[1] 'Regenerative Medicine - an overview | ScienceDirect Topics'. Accessed: Jun. 15, 2024. [Online]. Available: https://www.sciencedirect.com/topics/agricultural-and-biological-sciences/regenerative-medicine

[2] F. Berthiaume, T. J. Maguire, and M. L. Yarmush, 'Tissue engineering and regenerative medicine: history, progress, and challenges', *Annu. Rev. Chem. Biomol. Eng.*, vol. 2, pp. 403–430, 2011, doi: 10.1146/annurev-chembioeng-061010-114257.

[3] E. Jacques and E. J. Suuronen, 'The Progression of Regenerative Medicine and its Impact on Therapy Translation', *Clin. Transl. Sci.*, vol. 13, no. 3, pp. 440–450, May 2020, doi: 10.1111/cts.12736.

[4] J. Gao, X. Yu, X. Wang, Y. He, and J. Ding, 'Biomaterial–Related Cell Microenvironment in Tissue Engineering and Regenerative Medicine', *Engineering*, vol. 13, pp. 31–45, Jun. 2022, doi: 10.1016/j.eng.2021.11.025.

[5] H. L. Thomas and A. R. McClain, 'Optimization of Preparation Procedures for Manufacture of Vascular Implant Textiles', *J. Ind. Text.*, vol. 31, no. 1, pp. 57–73, Jul. 2001, doi: 10.1106/N079-25FG-JCVD-UC8Q.

[6] 'Processes | Free Full-Text | Advanced Biomedical Applications of Multifunctional Natural and Synthetic Biomaterials'. Accessed: Jun. 15, 2024. [Online]. Available: https://www.mdpi.com/2227-9717/11/9/2696

[7] D. Di Francesco, A. Pigliafreddo, S. Casarella, L. Di Nunno, D. Mantovani, and F. Boccafoschi, 'Biological Materials for Tissue-Engineered Vascular Grafts: Overview of Recent Advancements', *Biomolecules*, vol. 13, no. 9, Art. no. 9, Sep. 2023, doi: 10.3390/biom13091389.

[8] T. L. B. Ha *et al.*, 'Naturally Derived Biomaterials: Preparation and Application', in *Regenerative Medicine and Tissue Engineering*, IntechOpen, 2013. doi: 10.5772/55668.

[9] M. Brown, J. Li, C. Moraes, M. Tabrizian, and N. Y. K. Li-Jessen, 'Decellularized extracellular matrix: New promising and challenging biomaterials for regenerative medicine', *Biomaterials*, vol. 289, p. 121786, Oct. 2022, doi: 10.1016/j.biomaterials.2022.121786.

[10] H. Vilaça-Faria, J. Noro, R. L. Reis, and R. P. Pirraco, 'Extracellular matrix-derived materials for tissue engineering and regenerative medicine: A journey from isolation to characterization and application', *Bioact. Mater.*, vol. 34, pp. 494–519, Apr. 2024, doi: 10.1016/j.bioactmat.2024.01.004.

[11] S. Prete, M. Dattilo, F. Patitucci, G. Pezzi, O. I. Parisi, and F. Puoci, 'Natural and Synthetic Polymeric Biomaterials for Application in Wound Management', *J. Funct. Biomater.*, vol. 14, no. 9, p. 455, Sep. 2023, doi: 10.3390/jfb14090455.

[12] S. Samavedi, L. K. Poindexter, M. Van Dyke, and A. S. Goldstein, 'Chapter 7 - Synthetic Biomaterials for Regenerative Medicine Applications', in *Regenerative Medicine Applications in Organ Transplantation*, G. Orlando, J. Lerut, S. Soker, and R. J. Stratta, Eds., Boston: Academic Press, 2014, pp. 81–99. doi: 10.1016/B978-0-12-398523-1.00007-0.

[13] F.-M. Chen and X. Liu, 'Advancing biomaterials of human origin for tissue engineering', *Prog. Polym. Sci.*, vol. 53, pp. 86–168, Feb. 2016, doi: 10.1016/j.progpolymsci.2015.02.004.

[14] E. Insuasti-Cruz *et al.*, 'Natural Biomaterials from Biodiversity for Healthcare Applications', *Adv. Healthc. Mater.*, vol. 11, no. 1, p. e2101389, Jan. 2022, doi: 10.1002/adhm.202101389.

[15] S. Ullah and X. Chen, 'Fabrication, applications and challenges of natural biomaterials in tissue engineering', *Appl. Mater. Today*, vol. 20, p. 100656, Sep. 2020, doi: 10.1016/j.apmt.2020.100656.

[16] A. S. Tripathi *et al.*, 'Material matters: exploring the interplay between natural biomaterials and host immune system', *Front. Immunol.*, vol. 14, p. 1269960, 2023, doi: 10.3389/fimmu.2023.1269960.

[17] K. P. Robb, A. Shridhar, and L. E. Flynn, 'Decellularized Matrices As Cell-Instructive Scaffolds to Guide Tissue-Specific Regeneration', *ACS Biomater. Sci. Eng.*, vol. 4, no. 11, pp. 3627–3643, Nov. 2018, doi: 10.1021/acsbiomaterials.7b00619.

[18] S. Ricard-Blum, '"Regenerative medicine: Stem cells and extracellular matrix"', *Pathol. Biol.*, vol. 57, no. 4, p. 281, Jun. 2009, doi: 10.1016/j.patbio.2008.09.008.

[19] A. Porzionato, E. Stocco, S. Barbon, F. Grandi, V. Macchi, and R. De Caro, 'Tissue-Engineered Grafts from Human Decellularized Extracellular Matrices: A Systematic Review and Future Perspectives', *Int. J. Mol. Sci.*, vol. 19, no. 12, p. 4117, Dec. 2018, doi: 10.3390/ijms19124117.

[20] K. H. Hussein, K.-M. Park, L. Yu, H.-H. Kwak, and H.-M. Woo, 'Decellularized hepatic extracellular matrix hydrogel attenuates hepatic stellate cell activation and liver fibrosis', *Mater. Sci. Eng. C Mater. Biol. Appl.*, vol. 116, p. 111160, Nov. 2020, doi: 10.1016/j.msec.2020.111160.

[21] U. Mendibil, R. Ruiz-Hernandez, S. Retegi-Carrion, N. Garcia-Urquia, B. Olalde-Graells, and A. Abarrategi, 'Tissue-Specific Decellularization Methods: Rationale and Strategies to Achieve Regenerative Compounds', *Int. J. Mol. Sci.*, vol. 21, no. 15, p. 5447, Jul. 2020, doi: 10.3390/ijms21155447.
[22] S. Öztürk, A. E. Elçin, A. Koca, and Y. M. Elçin, 'Therapeutic Applications of Stem Cells and Extracellular Vesicles in Emergency Care: Futuristic Perspectives', *Stem Cell Rev. Rep.*, vol. 17, no. 2, pp. 390–410, Apr. 2021, doi: 10.1007/s12015-020-10029-2.
[23] H. H. Elmashhady, B. A. Kraemer, K. H. Patel, S. A. Sell, and K. Garg, 'Decellularized extracellular matrices for tissue engineering applications', *Electrospinning*, vol. 1, no. 1, pp. 87–99, Oct. 2017, doi: 10.1515/esp-2017-0005.
[24] A. Neishabouri, A. Soltani Khaboushan, F. Daghigh, A.-M. Kajbafzadeh, and M. Majidi Zolbin, 'Decellularization in Tissue Engineering and Regenerative Medicine: Evaluation, Modification, and Application Methods', *Front. Bioeng. Biotechnol.*, vol. 10, p. 805299, 2022, doi: 10.3389/fbioe.2022.805299.
[25] A. Gilpin and Y. Yang, 'Decellularization Strategies for Regenerative Medicine: From Processing Techniques to Applications', *BioMed Res. Int.*, vol. 2017, p. 9831534, 2017, doi: 10.1155/2017/9831534.
[26] M. Gadre, M. Kasturi, P. Agarwal, and K. S. Vasanthan, 'Decellularization and Their Significance for Tissue Regeneration in the Era of 3D Bioprinting', *ACS Omega*, vol. 9, no. 7, pp. 7375–7392, Feb. 2024, doi: 10.1021/acsomega.3c08930.
[27] Z. Chen *et al.*, 'Human decellularized adipose matrix derived hydrogel assists mesenchymal stem cells delivery and accelerates chronic wound healing', *J. Biomed. Mater. Res. A*, vol. 109, no. 8, pp. 1418–1428, Aug. 2021, doi: 10.1002/jbm.a.37133.
[28] J. Y. Hong, Y. Seo, G. Davaa, H.-W. Kim, S. H. Kim, and J. K. Hyun, 'Decellularized brain matrix enhances macrophage polarization and functional improvements in rat spinal cord injury', *Acta Biomater.*, vol. 101, pp. 357–371, Jan. 2020, doi: 10.1016/j.actbio.2019.11.012.
[29] J. W. Wassenaar *et al.*, 'Evidence for Mechanisms Underlying the Functional Benefits of a Myocardial Matrix Hydrogel for Post-MI Treatment', *J. Am. Coll. Cardiol.*, vol. 67, no. 9, pp. 1074–1086, Mar. 2016, doi: 10.1016/j.jacc.2015.12.035.
[30] W. Changchen, W. Hongquan, Z. Bo, X. Leilei, J. Haiyue, and P. Bo, 'The characterization, cytotoxicity, macrophage response and tissue regeneration of decellularized cartilage in costal cartilage defects', *Acta Biomater.*, vol. 136, pp. 147–158, Dec. 2021, doi: 10.1016/j.actbio.2021.09.031.
[31] S. Farnebo *et al.*, 'Design and characterization of an injectable tendon hydrogel: a novel scaffold for guided tissue regeneration in the musculoskeletal system', *Tissue Eng. Part A*, vol. 20, no. 9–10, pp. 1550–1561, May 2014, doi: 10.1089/ten.TEA.2013.0207.
[32] M. Ghetti *et al.*, 'Histological and ultrastructural evaluation of human decellularized matrix as a hernia repair device', *Ultrastruct. Pathol.*, vol. 42, no. 1, pp. 32–38, 2018, doi: 10.1080/01913123.2017.1365788.
[33] M. Parmaksiz, A. Dogan, S. Odabas, A. E. Elçin, and Y. M. Elçin, 'Clinical applications of decellularized extracellular matrices for tissue engineering and regenerative medicine', *Biomed. Mater. Bristol Engl.*, vol. 11, no. 2, p. 022003, Mar. 2016, doi: 10.1088/1748-6041/11/2/022003.
[34] L. Iop, A. Paolin, P. Aguiari, D. Trojan, E. Cogliati, and G. Gerosa, 'Decellularized Cryopreserved Allografts as Off-the-Shelf Allogeneic Alternative for Heart Valve Replacement: In Vitro Assessment Before Clinical Translation', *J Cardiovasc. Transl. Res.*, vol. 10, no. 2, pp. 93–103, Apr. 2017, doi: 10.1007/s12265-017-9738-0.
[35] E. Rieder *et al.*, 'Tissue engineering of heart valves: decellularized porcine and human valve scaffolds differ importantly in residual potential to attract monocytic cells', *Circulation*, vol. 111, no. 21, pp. 2792–2797, May 2005, doi: 10.1161/CIRCULATIONAHA.104.473629.
[36] P. Lm and W. Ra, 'Matrix-Bound Nanovesicles: What Are They and What Do They Do?', *Cells Tissues Organs*, vol. 212, no. 1, 2023, doi: 10.1159/000522575.
[37] N. J. Patel, A. Ashraf, and E. J. Chung, 'Extracellular Vesicles as Regulators of the Extracellular Matrix', *Bioeng. Basel Switz.*, vol. 10, no. 2, p. 136, Jan. 2023, doi: 10.3390/bioengineering10020136.
[38] G. S. Hussey *et al.*, 'Lipidomics and RNA sequencing reveal a novel subpopulation of nanovesicle within extracellular matrix biomaterials', *Sci. Adv.*, vol. 6, no. 12, p. eaay4361, Mar. 2020, doi: 10.1126/sciadv.aay4361.
[39] N. J. Turner, L. M. Quijano, G. S. Hussey, P. Jiang, and S. F. Badylak, 'Matrix Bound Nanovesicles Have Tissue-Specific Characteristics That Suggest a Regulatory Role', *Tissue Eng. Part A*, vol. 28, no. 21–22, pp. 879–892, Nov. 2022, doi: 10.1089/ten.tea.2022.0091.

[40] ‘Matrix-bound nanovesicles within ECM bioscaffolds | Science Advances’. Accessed: Jun. 14, 2024. [Online]. Available: https://www.science.org/doi/10.1126/sciadv.1600502
[41] L. M. Quijano *et al.*, ‘Matrix-Bound Nanovesicles: The Effects of Isolation Method upon Yield, Purity, and Function’, *Tissue Eng. Part C Methods*, vol. 26, no. 10, pp. 528–540, Oct. 2020, doi: 10.1089/ten.TEC.2020.0243.
[42] P. Subedi *et al.*, ‘Comparison of methods to isolate proteins from extracellular vesicles for mass spectrometry-based proteomic analyses’, *Anal. Biochem.*, vol. 584, p. 113390, Nov. 2019, doi: 10.1016/j.ab.2019.113390.
[43] M. Manfredi, S. Martinotti, F. Gosetti, E. Ranzato, and E. Marengo, ‘The secretome signature of malignant mesothelioma cell lines’, *J. Proteomics*, vol. 145, pp. 3–10, Aug. 2016, doi: 10.1016/j.jprot.2016.02.021.
[44] M. Kobayashi *et al.*, ‘Extraction and Biological Evaluation of Matrix-Bound Nanovesicles (MBVs) from High-Hydrostatic Pressure-Decellularized Tissues’, *Int. J. Mol. Sci.*, vol. 23, no. 16, p. 8868, Aug. 2022, doi: 10.3390/ijms23168868.
[45] M. C. Cramer *et al.*, ‘Extracellular vesicles present in bone, blood and extracellular matrix have distinctive characteristics and biologic roles’, *J. Immunol. Regen. Med.*, vol. 18, p. 100066, Nov. 2022, doi: 10.1016/j.regen.2022.100066.
[46] ‘The Extracellular Matrix, Growth Factors and Morphogens in Biomaterial Design and Tissue Engineering’. Accessed: Jun. 17, 2024. [Online]. Available: https://www.researchgate.net/publication/324508449_The_Extracellular_Matrix_Growth_Factors_and_Morphogens_in_Biomaterial_Design_and_Tissue_Engineering
[47] L. Maddaluno, C. Urwyler, and S. Werner, ‘Fibroblast growth factors: key players in regeneration and tissue repair’, *Dev. Camb. Engl.*, vol. 144, no. 22, pp. 4047–4060, Nov. 2017, doi: 10.1242/dev.152587.
[48] Y.-R. Yun *et al.*, ‘Fibroblast Growth Factors: Biology, Function, and Application for Tissue Regeneration’, *J. Tissue Eng.*, vol. 2010, p. 218142, Nov. 2010, doi: 10.4061/2010/218142.
[49] J. L. Labandeira-Garcia, M. A. Costa-Besada, C. M. Labandeira, B. Villar-Cheda, and A. I. Rodríguez-Perez, ‘Insulin-Like Growth Factor-1 and Neuroinflammation’, *Front. Aging Neurosci.*, vol. 9, p. 365, 2017, doi: 10.3389/fnagi.2017.00365.
[50] R. Nederlof *et al.*, ‘Insulin-Like Growth Factor 1 Attenuates the Pro-Inflammatory Phenotype of Neutrophils in Myocardial Infarction’, *Front. Immunol.*, vol. 13, p. 908023, 2022, doi: 10.3389/fimmu.2022.908023.
[51] Y. Dong, J. Zhong, and L. Dong, ‘The Role of Decorin in Autoimmune and Inflammatory Diseases’, *J. Immunol. Res.*, vol. 2022, p. 1283383, Aug. 2022, doi: 10.1155/2022/1283383.
[52] H. Kaur and S. M. Ghorai, ‘Role of Cytokines as Immunomodulators’, in *Immunomodulators and Human Health*, R. K. Kesharwani, R. K. Keservani, and A. K. Sharma, Eds., Singapore: Springer Nature, 2022, pp. 371–414. doi: 10.1007/978-981-16-6379-6_13.
[53] A. J. Lee and A. A. Ashkar, ‘The Dual Nature of Type I and Type II Interferons’, *Front. Immunol.*, vol. 9, Sep. 2018, doi: 10.3389/fimmu.2018.02061.
[54] ‘Role of Interleukin 10 Transcriptional Regulation in Inflammation and Autoimmune Disease - PMC’. Accessed: Jun. 17, 2024. [Online]. Available: https://www.ncbi.nlm.nih.gov/pmc/articles/PMC3410706/
[55] ‘IL-21 Proteins | Thermo Fisher Scientific’. Accessed: Jun. 17, 2024. [Online]. Available: https://www.thermofisher.com/proteins/target/il-21?gclid=Cj0KCQjwvb-zBhCmARIsAAfUI2tL7Lk-IVlSpRI3rdCTZY92HhpIUooknICRMfkh-7aUQEy2k_yK8eAaAgj1EALw_wcB&ef_id=Cj0KCQjwvb-zBhCmARIsAAfUI2tL7Lk-IVlSpRI3rdCTZY92HhpIUooknICRMfkh-7aUQEy2k_yK8eAaAgj1EALw_wcB:G:s&s_kwcid=AL!3652!3!666763205670!p!!g!!human%20interleukin%2021!20395796591!152475855078&cid=bid_clb_rep_r01_co_cp0000_pjt0000_bid00000_0se_gaw_rs_pur_con&gad_source=1
[56] ‘A guide to chemokines and their receptors - PMC’. Accessed: Jun. 17, 2024. [Online]. Available: https://www.ncbi.nlm.nih.gov/pmc/articles/PMC6120486/
[57] N. Karin and H. Razon, ‘Chemokines beyond chemo-attraction: CXCL10 and its significant role in cancer and autoimmunity’, *Cytokine*, vol. 109, pp. 24–28, Sep. 2018, doi: 10.1016/j.cyto.2018.02.012.
[58] C. Wang *et al.*, ‘Chapter 2 - Neural Cell Adhesion Molecules in Normal and Abnormal Neural Development’, in *Handbook of Developmental Neurotoxicology (Second Edition)*, W. Slikker, M. G. Paule, and C. Wang, Eds., Academic Press, 2018, pp. 17–22. doi: 10.1016/B978-0-12-809405-1.00002-X.

[59] H. H. Van Acker, A. Capsomidis, E. L. Smits, and V. F. Van Tendeloo, 'CD56 in the Immune System: More Than a Marker for Cytotoxicity?', *Front. Immunol.*, vol. 8, p. 892, 2017, doi: 10.3389/fimmu.2017.00892.
[60] X. Zhang, Y. F. Alanazi, T. A. Jowitt, A. M. Roseman, and C. Baldock, 'Elastic Fibre Proteins in Elastogenesis and Wound Healing', *Int. J. Mol. Sci.*, vol. 23, no. 8, p. 4087, Apr. 2022, doi: 10.3390/ijms23084087.
[61] D. Chanda *et al.*, 'Fibronectin on the Surface of Extracellular Vesicles Mediates Fibroblast Invasion', *Am. J. Respir. Cell Mol. Biol.*, vol. 60, no. 3, pp. 279–288, Mar. 2019, doi: 10.1165/rcmb.2018-0062OC.
[62] S. J. Popa, S. E. Stewart, and K. Moreau, 'Unconventional secretion of annexins and galectins', *Semin. Cell Dev. Biol.*, vol. 83, pp. 42–50, Nov. 2018, doi: 10.1016/j.semcdb.2018.02.022.
[63] 'IJMS | Free Full-Text | Exosomal Vimentin from Adipocyte Progenitors Protects Fibroblasts against Osmotic Stress and Inhibits Apoptosis to Enhance Wound Healing'. Accessed: Jun. 17, 2024. [Online]. Available: https://www.mdpi.com/1422-0067/22/9/4678
[64] A. Singh, S. Verma, S. B. Modak, M. M. Chaturvedi, and J. S. Purohit, 'Extra-nuclear histones: origin, significance and perspectives', *Mol. Cell. Biochem.*, vol. 477, no. 2, pp. 507–524, Feb. 2022, doi: 10.1007/s11010-021-04300-4.
[65] D. E. Heath, 'A Review of Decellularized Extracellular Matrix Biomaterials for Regenerative Engineering Applications', *Regen. Eng. Transl. Med.*, vol. 5, no. 2, pp. 155–166, Jun. 2019, doi: 10.1007/s40883-018-0080-0.
[66] M. J. Hernandez *et al.*, 'Manufacturing considerations for producing and assessing decellularized extracellular matrix hydrogels', *Methods San Diego Calif*, vol. 171, pp. 20–27, Jan. 2020, doi: 10.1016/j.ymeth.2019.09.015.
[67] T. D. Johnson *et al.*, 'Quantification of decellularized human myocardial matrix: A comparison of six patients', *Proteomics Clin. Appl.*, vol. 10, no. 1, pp. 75–83, Jan. 2016, doi: 10.1002/prca.201500048.
[68] E. I. Buzas, 'The roles of extracellular vesicles in the immune system', *Nat. Rev. Immunol.*, vol. 23, no. 4, pp. 236–250, Apr. 2023, doi: 10.1038/s41577-022-00763-8.
[69] 'Biomimicked Biomaterials Advances in Tissue Engineering and Regenerative Medicine: Advances in Tissue Engineering and Regenerative Medicine'. Accessed: Jun. 17, 2024. [Online]. Available: https://www.researchgate.net/publication/342546749_Biomimicked_Biomaterials_Advances_in_Tissue_Engineering_and_Regenerative_Medicine_Advances_in_Tissue_Engineering_and_Regenerative_Medicine
[70] R. A. Hortensius and B. A. Harley, 'Naturally derived biomaterials for addressing inflammation in tissue regeneration', *Exp. Biol. Med.*, vol. 241, no. 10, pp. 1015–1024, May 2016, doi: 10.1177/1535370216648022.
[71] R. J. Crum *et al.*, 'Biocompatibility and biodistribution of matrix-bound nanovesicles in vitro and in vivo', *Acta Biomater.*, vol. 155, pp. 113–122, Jan. 2023, doi: 10.1016/j.actbio.2022.11.026.
[72] L. Huleihel *et al.*, 'Matrix-Bound Nanovesicles Recapitulate Extracellular Matrix Effects on Macrophage Phenotype', *Tissue Eng. Part A*, vol. 23, no. 21–22, pp. 1283–1294, Nov. 2017, doi: 10.1089/ten.TEA.2017.0102.

8. ACKNOWLEDGEMENTS

I would like to express my heartfelt gratitude to my Prof. Boccafoschi Francesca for giving me the incredible opportunity to work under her guidance. Her unwavering enthusiasm and kindness made me feel truly welcome creating an environment where I could grow and learn with confidence. I am deeply thankful for all the knowledge she has shared with me. I cannot thank enough for the opportunities she has provided and the significant contribution to both my current studies and future endeavors. Thank you.

I would like to thank Tissuegraft srl that financed this project. This thesis project was partially financed by NODES which has received funding from the MUR-M4C2-1.5 of PNRR with grant agreement no. ECS00000036.

I would like to thank the whole Anatomy Laboratory for making this experience amazing, fun and this project would not have been possible without the collective efforts and unwavering commitment of each team member.

I am immensely grateful to Dalila for her tireless efforts. Her diligence, creativity, and collaborative spirit have not only enhanced the quality of our work but also made the journey enjoyable. Thanks for your infinite patience, for always being there when I was in need. In you, I have not only found a great tutor, but also a great friend.

Thanks to Simona for the encouragement, support and friendship. They are invaluable to me.

Thanks to all my colleagues: Edoardo, Federica, Irene, Alberto, Francesca and Fabiana. These past two years have been full of laughter, fun, hard work and unforgettable memories.

To my parents, thank you for your endless love and encouragement. Your belief in me has been a constant source of strength and motivation. Your sacrifices and support have made all of this possible, and I am forever grateful.

To my brother, thank you for always being there for me. Your love and humor have made the tough times easier and the good times even better.

To Stefano, thank you for your unwavering support, patience, and love. Your belief in me and your encouragement have been invaluable, I couldn't have done this without you.

Thank you all for being my pillars of strength and for making these years unforgettable.